Energy

Assessment of Latvia's renewable energy supply-demand economic potential and policy recommendations, VPP-EM-2018/AER-1-0001

INTEGRATING A SYSTEM DYNAMICS MODEL WITH A GIS STRUCTURE

Integrating a system dynamics model with a GIS structure, 2021, 48 pp.

Authors
Andra Blumberga, Dr.sc.ing.
Dagnija Blumberga, Dr.habil.sc.ing
Silvija Nora Kalniņš, Dr.sc.ing.
Ruta Vanaga, Dr.sc.ing.
Ieva Pakere, Ph.D.
Zane Indzere, M.sc.ing.
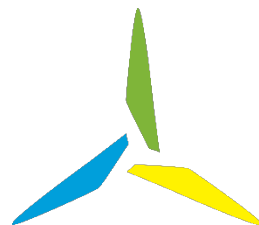**Armands Grāvelsiņš, M.sc.ing.**
Ketija Bumbiere, M.sc.ing.
Marika Kacare, M.sc.ing.
Antra Kalnbaļķīte, M.sc.
Ilze Vamža, M.sc.
Alise Ozarska, M.sc.
Terēza Bezručko, B.sc.

CONTENT

Abbreviations

ATVK – Classification of Administrative Territories and Territorial Units
DH – district heating
ETS – Emission Trading System
GIS – Geographic Information System
GUI – Graphical User Interface
IDE – Integrated Development Environment
KPR – Kurzeme Planning Region
LĢIA – The Latvian Geospatial Information Agency
LPR – Latgales plānošanas reģions
LVĢMC – The Latvian Environment, Geology and Meteorology Centre
NECP – National energy and climate plan
OIK – Mandatory procurement component
RES – Renewable Energy Sources
RPR – Riga Planning Region
SD – System Dynamics
VID – State Revenue Service of the Republic of Latvia
VPR – Vidzeme Planning Region
ZPR – Zemgale Planning Region

INTRODUCTION

To fully assess the potential for integrating renewable and local energy sources into the energy system, it is necessary to analyse the operation of the energy system as a whole and its development dynamics. Elements of the energy system, such as policy-making, infrastructure expansion, market behaviour, environmental impact and security of supply, are interlinked, so it is impossible to analyse one part of it, such as energy production, transmission or consumption, separately. RES modelling tools need to identify, for example, the reserve capacity required to integrate an increasing share of renewable energy sources, assess infrastructure investments to transport energy to other regions, study energy and climate policy issues, and identify regulatory frameworks for the energy market development. In addition to these dimensions, the assessment of energy transition requires more extensive modelling that considers the impact of short-term aspects of network stability and energy markets on long-term decarbonisation strategies.

Modelling is transforming those complicated systems into something we can understand and influence. Models that are too simple provide a lack of insight; however, the ones too complex require too much data, not to forget that the chances for the error are higher with every additional parameter. The System Dynamic (SD) approach is an effective tool to predict processes' behaviour, but it lacks the crucial spatial component for nature-related issues. Geographic Information Systems (GIS) provides this missing part by visualising the current or predicted situation and interpolating the data to areas where measurements were not made. SD and GIS represent distinct spheres of analysis; the combination provides new tools for many scientists and policymakers involved in environmental problem-solving.

No country is homogeneous, and remembering it helps identify the specific source of the problem, meaning it can optimise the effort needed to solve it, saving time and resources. In Latvia, most data sets, especially those collected and processed in a centralised way for the whole country and those publicly available, are generalised for the entire territory. Often, regional governments contain and publish data at the local level. Still, this process lacks guidance, so data is available mainly due to local government voluntary initiatives to attract investors or tourists or publicity requirements for funding projects. Regional decision-makers need to assess which technologies offer the best economic potential in specific local conditions and the available energy resources to use more effectively. Relying on national impact assessments is not due to particular local and regional circumstances.

Here, SD helps to understand all the links between resource availability, technological development, policy, economic benefits, and other factors and estimate the potential changes by changing these factors. The GIS should represent these relationships spatially - supposedly in an interactive map that depicts changes by changing factor values in a system dynamics model. To assess the spatial limitations of the power system, local differences and RES potential more accurately in different regions of Latvia, the SD modelling tool has been supplemented with a GIS modelling method used for both input data acquisition and spatial visualisation of results. The report provides an overview of connecting the SD model and the GIS system.

1. THE SPATIAL DIMENSION OF THE SYSTEMS

Most systems involved in natural processes depend not only on the interaction of elements in time but also in space. In this context, energy production from local and renewable resources can be cited as one of the most striking examples. It is characterised by many spatially variable elements, such as biomass availability, wind speed, solar radiation, location of production facilities, transmission network infrastructure, regional energy demand, etc.

Including time and space as additional parameters are not enough to model the energy system. They need to be fully integrated into the model to understand their dynamics, such as energy demand, fossil and renewable resource availability and efficiency, energy infrastructure capacity and load, decentralised energy storage, and, finally, return on investment and economic viability [1].

At present, external assumptions about macro-level indicators are mainly used to represent the energy system. To assess, for example, energy consumption over time, scale is one of the main prerequisites. Depending on it, the hourly load curve can be very different, but at the same time, it can represent a smoothing effect in case of increasing the system limit. The number and type of elements of the spatial and temporal dimension can have significant technical, financial, and environmental impacts, determined by the infrastructure network, the chosen alternatives, the technologies, and other factors. The reciprocal allocation of resources is linked to economic, political, and social issues. These links must be considered when analysing the availability of resources and developing policies. Depending on the specific energy system in a given area, solutions to reduce system and cost risks may include, for example, centralised rather than a distributed generation (or both) or the extension of transmission networks, rather than the introduction of several autonomous alternatives [2].

Predicting future processes is difficult because there are several methods for estimating and modelling, on the interpretation of which the results depend. Calibration of the model is necessary to determine the values of parameters for which insufficient data have been obtained after measurements. Calibration and verification are mainly based on historical information, as past trends are likely to recur in the future. The usual method is to split the data into calibration and verification data packets. Calibration determines the most appropriate values for unknown parameters by modifying them to fit the model best. Predictions are checked during verification. Calibration based on historical data will only be valid if the process's conditions remain unchanged [3].

Another way to evaluate the validity of a model is to assess each of its components separately. Sensitivity analysis is usually performed to determine the most influential parameters. Each parameter is systematically changed to observe the effect on the result. For example, the model is run three times - with the parameter's actual value decreasing by 10% and increasing by 1%. If the results differ by less than 10%, the significance of the parameter is not critical. Accordingly, the accuracy of the data for a particular parameter is not a significant concern. Some parameters are essential and special attention must be paid to the information they contain [3].

RES is often seen as a crucial component of energy independence and security, as resources such as solar and wind cannot be affected as quickly by global policies and market strategies as gas or oil products. However, although RES can be a cheap energy source, the total cost depends on the technology used, so the market situation matters. Depending on where the equipment and its components are manufactured, SD tools can also model changes in these factors. Sandor [4] created a global trade model for high-purity polycrystalline silicon. Polycrystalline silicon is the primary material of solar photovoltaics. It has undergone significant price changes, which have affected the production volume and costs of solar panels. Using STELLA, they developed and tested the model in China, the United States and the rest of the world, using Chinese historical data for verification [4].

Carbon reduction policies are relevant worldwide, and modelling as part of planning is vital for fast-growing economies like China. Without a prior assessment, it is impossible to implement an effective policy if the gross domestic product and the stock market grow several times every few years. SD modelling and demonstrating the long-term benefits of changing energy consumption patterns is a way to implement RES without significant economic losses [5].

1.1. Spatial GIS modelling

Spatial and temporal resolution determine the relationship between the actual process and the model that characterises it. They will never be identical, so uncertainty must be considered. There are different types of models. The model can be discrete or continuous, individual or aggregated. Models can be static or dynamic if the output data describes a later period than the input data and feedback. Static models mainly contain indicators such as layers of mapped information on topographic indicators, soil quality, agricultural practices, and other properties to assess erosion. Dynamic models represent a process that changes or transforms an aspect of the earth's surface over time. Weather forecasts are an example of a dynamic model. GIS is a handy tool for incorporating a spatial component into all types of models [3].

There are two types of GIS models. In one case, the model is a set of predicted data, such as an attribute table, which summarises the parameters characteristic of a real object (for example, for a lake, they would be depth, area, type). This sample can easily describe things objects and their characteristic data. In the second case, the model shows one or more processes, such as the direction of erosion or the affected areas [3].

While GIS is the best way to show spatial change, it is more challenging to change over time. Visualising time on a map often involves dividing a region into smaller areas, creating many basic units. Choosing the correct basic unit is crucial to avoid generalising the territory. Another approach is to track the locations of moving objects by recording the condition of rocks depending on erosion. The third way is to show the time change as a simple sequence of snapshots for each period. [3].

2. COMBINING SYSTEM DYNAMICS AND GIS MODELLING

SD was created as a non-spatial system modelling tool. Attempts to integrate the spatial dimension into SD have resulted in developing programs such as the *Spatial Modeling Environment (SME)* and *SIMILE*. The *SME* spatial relationship is transferred to the *STELLA Architect SD* modelling environment by transforming the *STELLA Architect* output data into *C ++* code, compiling it, and running it at the selected runtime, representing the SD model spatial network. One such model is the *Great Bay* model, which is based on a model developed in the *STELLA Architect* program to represent the variability of carbon flux in the Great Gulf ecosystem in New Hampshire. The model uses a cell size of 100 x 100 m^2, where each cell has a copy of the basic model, initialised with cell-specific values [6]. Additional tools such as *SIMARC* and *5D* have been developed to address the shortcomings of SD in spatial process modelling. Well-designed concepts and appropriate software have enabled spatial SD in various fields, mainly in studying specific issues such as ecosystem modelling, hydrology and invasive species control. Most of these models focus on spatial propagation processes. Meanwhile, very little attention is paid in the spatial SD to the simulations of the structures that characterise the arrangement and interrelationships of the system elements.

The structural change model deals with the change of spatial structures over time and the processes that cause these changes. One example of such a model is the land cover model. Land cover is determined by the properties of the earth's surface and the surface underground, which are transformed over time by natural and anthropogenic processes. The spatial arrangement of the elements influences these processes. So far, this type of feedback has been introduced in spatial SD by some modellers [7]. SD equations are sometimes integrated into the GIS model when adding spatial data to SD models. This approach fails to display the spatial component correctly, so programming must be used [8].

There are several reasons for combining SD and GIS. When creating a model for solving environmental problems, it is essential to preserve the spatial representation. GIS allows you to analyse the spatial aspects of a problem. However, it does not provide sufficient detail to study the structure of causation underlying such issues. In addition, the GIS representation is static. SD modelling allows the GIS model to improve these shortcomings. GIS can offer better visualisation tools as well as spatial analysis. Combining the two methods makes them more comprehensive [8].

These methods are linked in environmental science, engineering, and anywhere else where spatial analysis is required. The most popular area is hydrology, especially flood control. The systems covered by the SD methodology are dynamic. Their components interact closely with each other, are time-dependent and often contradictory. The causes and effects are not linked, and it isn't elementary to quantify the impact. For example, publications mention flood control, where the construction of dams can cause more severe flooding, impeding the natural discharge of excess water into floodplains [8].

When modelling energy systems, the inclusion of time and space in the form of additional parameters is not always sufficient [1]. Time and space need to be integrated into the model to understand better the dynamics of energy demand, the availability and efficiency of conventional and renewable resources, the capacity and load of energy infrastructure, decentralised energy storage and return on investment and profitability. Geographical conditions are an essential factor that should not be overlooked when natural or social processes are observed. Location and specific details are primarily included in research on a larger scale, such as international or global differences, but they also affect the national level [9].

The potential of GIS statistical modelling has been greatly enhanced due to graphical accessibility, which allows the user to interact with different stages of the modelling process. However, there are still problems with GIS with dynamic modelling. Programming languages that

provide feedback help in this regard. ArcGIS currently allows you to write scripts in standard languages such as *Microsoft Corporation Visual Basic for Applications*, *Python* un *PERL* [3].

There are different SD connections to GIS: built-in connection, tight connection, and weak connection. A close relationship is mainly based on dynamic data exchange. The link between SD and GIS can be achieved through a spreadsheet by transferring data from SD to GIS. Updating results in GIS is not yet fully automated [8].

The easiest way to combine the two methods is to use GIS to create SD-based maps without returning results to the model. In the example of Stuttgart [10], a detailed SD model was developed, containing the structure of all major cities, describing the parameters in four sectors (buildings, economic performance, society and environmental aspects), with a particular focus on buildings. Building files were created based on the model and analysed using the GIS tool. In this study, GIS does not provide feedback to SD, but both tools significantly improve the analysis.

The *STELLA Architect* SD program supports dynamic modelling and has the advantage of a visual design that helps show processes and causal relationships in simple diagrams. It can be connected to GIS.

Visual *C++* algorithms have been used to develop a global flow model, but there are limitations, such as that they cannot be modified during the simulation and are not interactive. Recent attempts to improve these algorithms have used *Vensim* model files for the SD part [11].

One type of combination is the addition of cellular automata to connect SD and GIS. There is no limit to the number of dimensions. The cellular automata are used in biology, geography and ecology to model and extensively visualise spatially distributed processes. For example, it can simulate urban development or the spread of forest fires. This is one of the oldest methods described in the scientific literature, allowing the spatial and temporal distribution of model processes. However, it is a simple approach with its limitations. It is challenging to include global parameters that affect the whole model, and it must be borne in mind that changes are rarely consistent over time. Integration with GIS solves some of these issues. The cellular automata work better for event simulation than for continuous process simulation, as it provides uniformity, universality and process regularity. In addition, the behaviour of a cell is assumed to be strongly related to adjacent cells [12].

Often during interactivity, SD interactivity is lost, and no changes can be made during simulation. A cellular automaton is one way to solve this problem. In this case, the SD model is based on spatial cells of the required resolution. The data exchange between SD and GIS is dynamic. It provides feedback from SD to GIS and vice versa. Modelling spatially distributed dynamic processes requires preparing and analysing vast amounts of spatial data, and GIS is helpful in this regard. Not only does it help to visualise the results, but it also serves to store spatial data. [8].

The *Python* programming language connects the *Vensim* SD modelling program to *ArcGIS*. The merge script uses DLL files (.dll), library files (.lib), model files (.vpm), and raster GIS database files (.mdb) to link the Vensim model and GIS tools dynamically. The algorithm of the work is as follows: the SD model is loaded, during the whole simulation, it is possible to control the parameters of the model to obtain as complete information as possible. If SD did all the simulation before transferring the results to *Python*, the interaction between GIS and SD would not be possible. If done correctly, *Python* creates a dynamic connection between the two software tools [8].

Unique values are used in the code that performs GIS calculations, but GIS data is mainly stored and passed to the code as raster files, so the parameter information must be converted to values that the code can perceive. The resulting values can be used to calculate the required parameters using programming tools such as *Python* or returned to the SD model. In one example, the computation is organised as follows: a GIS raster file describing the population is generated (predefined ranges range from 0 to 5); the distance from the hospital to each raster

cell of the simulation domain is calculated; travel costs are calculated based on distance; the population served by each hospital is estimated by finding the sum of the values of the population; the calculated values are returned to the *Vensim* model. Modelling is continued using the new values [8].

STELLA uses two *Python* libraries to translate the *.xmile* file created by *STELLA: PTSD* [13] *and BTPK_Py* [14]. Both are open source solutions and are available via the pip install for installing *Python* libraries. However, both require *Python* skills. The programming languages evaluated for connection are *C ++*, *Java*, and *Python*. These are all open-source, object-oriented languages. While other options are based on *ESRI* recommendations, *Python* best works best with *ArcGIS*. ESRI provides free online courses and documentation that greatly facilitate connectivity. TIn addition, *Python* and *ArcGIS* integration runs in the background because *ArcPy* already has built-in *ArcGIS Pro*. This allows much of the GIS functionality to be converted to *Python* code [15], [16]. *Python* Python is compatible with both *STELLA* and *ArcGIS*. *ESRI* promotes it as the primary GIS scripting language. *Python* supports *Vensim* better, although it is also possible to work with *STELLA* models [15].

The latest versions of *Python* can be used, but scientists (*Peck, Neuwirth* un *Simonovic*, 2014) say version 2. x (x stands for subversion number) may have better support for the *ArcGIS* package and library. These libraries are currently out of date. It is also possible to convert files to R code using *Python* scripts [17].

3. METDOLOGY OF MODEL COUPLING

The methodology (Fig. 3.1) consists of data acquisition for the SD model and input data analysis. Spatial analysis has been used to fill in data gaps where necessary by identifying the area potentially available for wind energy production. Various databases have been studied to find the information required to describe the influencing factors from all influential perspectives, including taxes and policies.
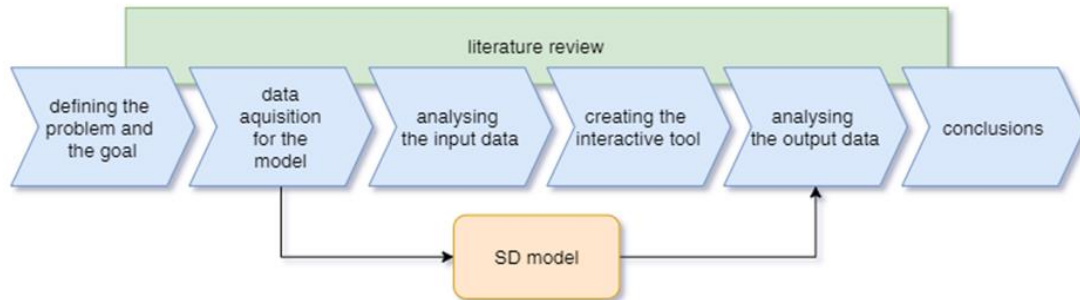

Fig.3.1. Model connection methodology

The connection of SD and GIS models developed to assess RES potential occurs in two stages (Figure 3.2). The GIS model obtains the necessary input data to create the SD model in the first stage. In the second stage, the results of the SD model are spatially visualised using a GIS platform.
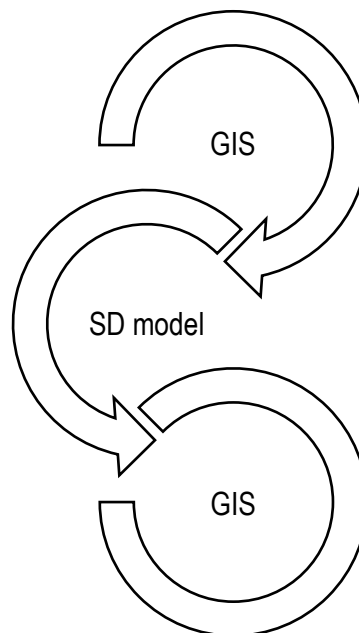
Fig.3.2. Linking SD and GIS models

The SD model was used, described in the report "Structure of the System Dynamics Model. Output data and mathematical relations". Model output converted to *.js* files. The visualisation tool was created using *JavaScript*. It is easily customisable for display according to user needs, making it easier to compare regions. The literature review was performed to confirm the assumptions about the chosen methodology.

It is crucial to identify existing fossil energy and RES energy sources to assess the development potential of renewable energy in Latvia. Given that the possibility of renewable

energy sources is affected by spatially changing conditions, it is appropriate to use a mapping method for this purpose. The resulting regional profiles and defined constraints for a particular RES can be used in modelling tools such as SD modelling, linear programming models, etc.

The detailed spatial analysis workflow of the study (Figure 3.3) shows the databases used for the SD model. Various information databases (Latvian geographical information, Wind Atlas, Latvian State Forest Database, etc.) and data analysis methods have been used to determine the spatial profile of Latvian RES potential, heat and energy production and consumption.

Household electricity consumption, wind energy and regional breakdown data are processed using *ArcGIS*.
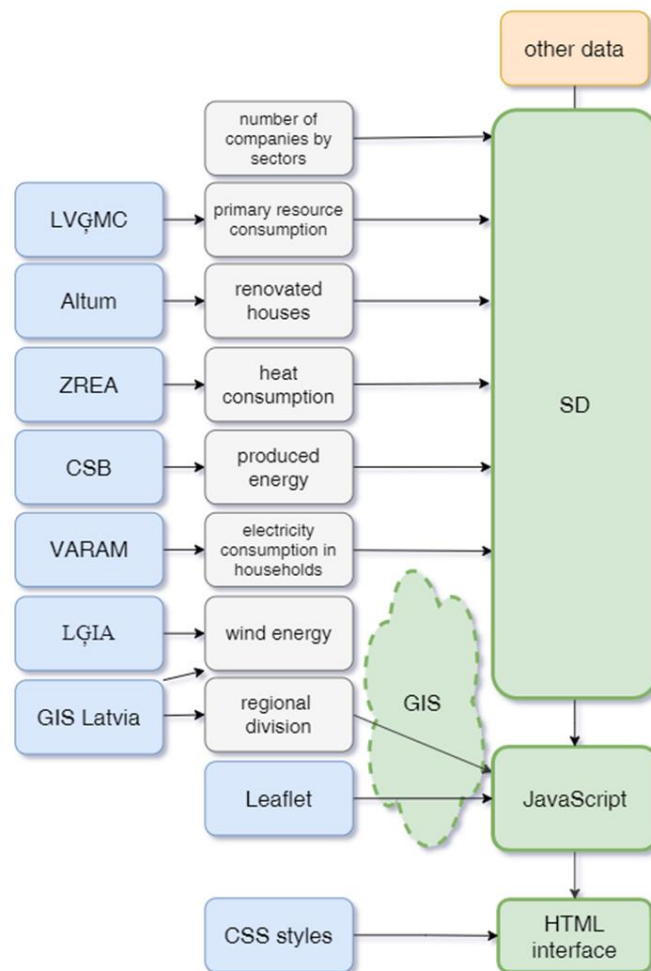
Fig.3.3. Research algorithm

The study consists of several stages.

Model validation. Multi-year data (2012-2017) have been collected for verification, thus preventing year-specific data from affecting the model. Most data for the entire period are not available, and assumptions have been made based on public information.

Parameter matching between SD model and GIS functionality; Convert file formats to a tool-readable format. The SD model generates a *.csv* file converted to a *.js* file using a *Python* script to use the data in *JavaScript* code. The original model file contained Latvian characters and commas as a decimal separator, which was changed to fit the file's code.

Creating a visualisation tool. A user interface visualises data created using *HTML* and *JavaScript* with *CSS* styles. *OpenStreetMap* is used as the base map. The map shows the differences between the regions.

Evaluation of results and adaptation to the needs of the broader scope of the project. The analysis at the regional level provides a simplified insight into the distribution of resources in Latvia and can help plan development at the regional level. In the light of the forthcoming regional reform, analysis at the regional level will be critical.

The results of the two software are combined through programming to achieve this goal. The SD model is created using *STELLA Architect* version 2.0.1.with *ISEE* systems. The cartographic part is made in *ArcGIS Pro* 2.6.0, designed as an *ESRI* and *JavaScript* library brochure (Table 3.1).

VS Code is used as an IIV because it works with most software, so it is unnecessary to change the IIV using different languages.

Table 3.1

Software used

Software	Version	The aim
MS Excel	2106	Data storage and calculations
STELLA Architect by isee systems	2.0.1.	Creating an SD model
ArcGIS PRO by ESRI	2.6.0.	GIS data analysis
VS Code	1.55.2.	IIV programming part
JavaScript	V8	Script data selection
Leaflet	1.7.1.	Cartographic elements GLS
Python	3.8.	Data formatting
HTML	5.3.	Establishment of GLS
CSS	2.1.	GLS style setting

3.1. Use of GIS to identify input data

It is essential to identify the spatial distribution of resources to plan the territorially unified development of renewable energy and, consequently, the efficient use of resources. This subsection analyses the spatial distribution of the primary local and renewable energy resources. It is based on the municipal level (counties and republican cities) and the regional level (statistical regions). The analysis at the municipal level provides an opportunity to assess the unique opportunities of each municipality to use the resources available in it, as well as to judge the potential opportunities for cooperation with neighbouring cities. In turn, the analysis at the regional level provides a simplified insight into the distribution of resources in Latvia and can help regional plan development.

3.1.1. Energy sector overview by region

The competencies of the planning region ensure regional development planning, coordination, cooperation between local governments and other public administration institutions. In addition, the planning regions determine the main basic principles, goals and priorities for the long-term development of the planning area. Their purpose is to coordinate regional development planning by action planning documents, manage and supervise the development and implementation of planning programs and spatial plans, and ensure the evaluation and coordination of regional and local level development planning documents and compliance with regulatory enactments. Planning regions establish cooperation between local governments and state-level institutions [18].

To implement the regional competence of planning, the Development Council of the Planning Region approves the regulations and budget of regional planning; it may establish or

reorganise regional planning institutions and capital companies and decide on membership in associations and foundations [18].

Kurzeme planning region

KPR is exploring the potential of oil extraction. According to local authorities, the region should develop underground gas storage facilities. Due to the development opportunities of wind energy, the construction of a new 330 kV line is planned. A new gas connection with Ventspils is expected. KPR is an underground gas storage facility used for pan-European gas storage [19].

Kurzeme has significant resources for developing wind energy in the western and highland areas. There is potential for the growth of solar energy in coastal areas. The southwestern part of the region has the resources to develop geothermal energy, reaching temperature gradients of 50-60 °C at a depth of 1 km. [19].

Latgale planning region

No publicly available data for the region.

The Latvian Environmental Investment Fund has several projects related to the energy sector: "Promoting the availability of energy data in 5 municipalities of the Latgale planning region". Many other projects are planned at the national level, such as "the Promotion of Bioenergy 2", including the LPR [20].

Riga planning region

Natural gas systems have the largest installed heat capacity in the region, accounting for 89% of the installed capacity. The largest installed heat capacities are in the Salaspils region and Riga, where TEC-1 and TEC-2 are located. The largest hydroelectric power plants in RPR are the Riga HPP and the Kegums HPP, with 402 MW and 264 MW, respectively. The total installed capacity of 17 small hydropower plants is 2614 MW. The total share of Riga HPP and Ķegums HPP in RPR is 60.1% and 39.5% [21], [22].

The most common solid biomass fuel RPR is wood chips (88% of total substantial biomass consumption in the region). Firewood consumption is 6%. Riga consumes almost 64% of the total consumption of wood chips. Riga's energy supply is crucial in the country's energy sector [21].

There is currently only one wind farm in the RPR area. There, the wind speed at an altitude of 50 m is the highest in the region. Elsewhere, the potential for wind energy is lower, so wind energy is not currently a priority. The total installed wind power capacity RPR is 1.2 MW. The Vidzeme Biosphere Reserve must be considered [21].

RPR's largest solar power plant is in Riga and belongs to SIA EKO OSTA and Salacgrīva. Different areas are considering starting to install solar panels. There are RES combination practice cases in the Sigulda region when solar energy is used with a pellet boiler [22].

Vidzeme planning region

The three most extensive energy production facilities in the region use natural gas. Increasingly, natural gas is being at least partially replaced by RES, such as biomass, in DH systems. This is facilitated by various support programs specifically for DH systems, aiming to promote RES, increase energy efficiency and reduce dependence on fossil fuels. Biomass is widely used, especially for boilers with a heat output > 0.5-1 MW and relatively low capacity DH systems. Other renewable energy sources (hydropower, wind power and solar energy) are rarely used, mainly in private or municipal facilities such as solar panels for heat production [23].

About 60% of all buildings were built between 1960 and 1990. About 80% of these buildings do not meet the minimum energy efficiency requirements and have a relatively low thermal resistance. Due to the relatively low level of income of the population, the amount of

investment required and a sufficiently long payback period, the renovation of these buildings and the improvement of energy efficiency are slow. The energy expenditure share in the region's households is 9.9% of income [23].

Zemgale planning region

Every year the total number of boiler houses in ZPR decreases. In 2009, ZPR operated 113 boiler houses; In 2017, their number was 82. The number of cogeneration plants has increased from 11 cogeneration plants in 2009 to 44 cogeneration plants in 2017 [24].

The amount of heat produced by RES is increasing every year. In 2013, 73.2% of the heat produced was imported fossil energy resources, mainly natural gas. However, in 2016, 72% of the energy produced was generated from RES (542.90 GWh out of 752.21 GWh), mainly from wood chips, biogas, firewood, wood processing residues etc.). The rest is fossil energy resources [24].

The most pressing issue is obsolete individual boilers and systems, which result in high heating costs. In some municipalities, such as Jelgava, Dobele, and Sala, the share of fossil fuels is still high. This is a crucial issue due to poor fuel quality control. The proportion of renovated apartment buildings is insufficient to meet energy efficiency standards [24].

Sparsely populated apartment buildings in the villages of the region (Aknīste, Viesīte, Pļaviņas, Krustpils) make it challenging to create centralised solutions. In Aizkraukle, Pļaviņas and Jēkabpils municipalities, more than 20% of municipal buildings have been renovated [24].

The average electricity consumption per capita in ZPR is slightly lower than the average in Latvia - 823 kWh per capita [24].

Table 3.2 shows that KPR has the most significant potential for different RES, but ZPR has considerable potential for agricultural waste resources such as manure and straw. LPR and VPR have a lower potential for RES, which indicates the need for cooperation with other regions to increase the overall share of RES.

Table 3.2

Overview of average RES potential [25]

	Kurzeme	Latgale	Riga	Vidzeme	Zemgale
The intensity of solar radiation, kWh/m^2 per year	1180	1149	1155	1121	1154
Wind speed, m/s per year	7.2	7.1	7	6.9	7.1
Low-quality wood, t/km^2 per year	1908	1259	1905	1895	1493
Manure resource, dry matter t/km^2 per year	16	14.1	17.1	13.9	35.4
Straw resources, dry matter t/km^2 per year	18.7	11.5	12.5	9.7	32.2
Sewage sludge resources, t/km^2 per year	0.17	0.26	0.35	0.27	0.18

3.1.2. Evaluation of RES potential

The GIS model has been used to identify renewable energy potential in planning regions. The primary resources for developing renewable energy are solar energy, wind energy, and several bioresources - sewage sludge, manure, straw and wood. Considering the relatively broad distribution of bogs in the territory of Latvia, the chapter also examines the distribution of peat as a local energy resource. Assuming that Latvia's most significant hydropower potential is already being used [26], this study does not consider the broader use of hydropower. Algae are also regarded as potential resources in energy; however, because their resources are challenging to identify and there are opportunities for their cultivation, algae has not been assessed spatially as a resource in this study. Household waste is also a promising renewable energy source, but given the limited availability of spatial data by type of waste and the fact that energy recovery

from waste is still one of the most expensive forms of energy recovery [27], the spatial distribution of waste as a resource is not analysed in this chapter.

- To characterise the spatial potential of wind energy in Latvia, data on the average wind speed in statistical regions and municipalities have been compiled. The data were obtained from the *Global Wind Atlas* [28], developed by the Technical University of Denmark and the World Bank Group, using climatic wind data from 2008-2017. Considering the current wind turbine heights, this study uses data on wind speeds at an altitude of 100 m.
- Data from the European Commission's Photovoltaic Geographic Information System (PVGIS) have been used to judge the differences in solar irradiation between Latvia's statistical regions and municipalities [29]. Annual data on irradiation in the plane at an angle of incidence of 35 ° are used to express solar energy resources. Data on the produced sewage sludge were obtained from the Latvian Environment, Geology and Meteorology Center "2-Ūdens" summary for 2018 [30]. The amount of sludge is expressed in dry matter.
- Data on the amount of manure were obtained using data from the public database of the Agricultural Data Center on the number of animals in municipalities in 2019 [31]. Data on manure from cattle and pigs have been used in the calculations, given that manure from these animals is used most for biogas production. To calculate the amount of manure obtained, the information on manure yield per animal included in the national standard "Manure extraction and management" of the Ministry of Agriculture of the Republic of Latvia has been used (Latvijas Republikas Zemkopības ministrija, 2008). The classification of manure given in that document was used to calculate the dry matter content. Solid litter manure is manure with a dry matter content of at least 15% for this classification. In contrast, liquid manure is any mixture of solid excrement, urine and water with a dry matter content of between 3% and 8%. Therefore, the lowest possible dry matter values (15% and 3%, respectively) were used in the calculations.
- Data on straw yield was calculated using the data of the Rural Support Service on the area of cereals in 2018 [33] and the data of the Central Statistical Bureau on the average yield of grains in the counties in 2018 [34]. Calculations are based on oats, wheat, barley, rye, triticale, and buckwheat results. Data on oats, wheat, barley, rye and triticale [35] and buckwheat [36] available in the scientific literature were used to determine the grain-straw ratio. At the same time, data on moisture content were taken from the European Commission's Joint Research Centre's expert consultation protocol "Cereal straw resources for bioenergy". In the European Union " [37].
- Data on the amount of stock in the counties were obtained from the Forest Statistics of the State Forest Service for 2019 [38]. Based on the information provided in the literature, it is estimated that low-quality wood (branches, bark and foliage) accounts for about 40% of the total stock [39].

The obtained results of spatial analysis of RES potential in different planning regions are discussed in the handover of this project on the used SD model input data values.

3.1.3. Identification of RES constraints

After determining available RES and energy consumption, the authors have identified the possible limitations for wind energy use. This resource is highly influenced by the land availability for wind turbine installation. Authors assume that solar technologies could be mainly installed on the rooftops of buildings; therefore, land ability is not a primary barrier to using solar energy.

During the research, ESRI ArcGIS Pro software and open-source data are used to spatially estimate which locations should be considered first for the wind park constructions considering primary legal limitations such as the regulated buffer zones around various objects and territories, technical limitations of buildings, and the possibility to use and transfer the energy

According to the Global Wind Atlas (Technical University of Denmark, World Bank Group, bez datuma), there is no territory with an average wind velocity lower than three m/s, so no domain was excluded based on this factor. The average wind speed of about seven m/s is assumed. The regional differences are insignificant but might play a role in further calculations where turbine parameters are predefined.

During the research, the main factors affecting the geographic availability of wind energy were estimated. To perform the evaluation based on the various influencing parameters, they were divided into two groups – the biding limitations and the limitations that entail additional technical difficulties that are possible to bypass with the extra costs.

The data layers available from ArcGIS Pro and Envirotech from the GIS Latvia 10.2 database, regularly updated, were used to determine the approximate area open in each planning region (Table 3.3).

The layers of buildings are taken from the GIS Latvia 9.2 database. Buffer zones were created around towns (2 km) and villages (1 km). All cities are available as a point layer. However, the area is also open in the county layer for the largest ones. In these cases, a buffer was created around the city territory.

To determine the area, buffer zones have been established around towns (2 km) and villages (1 km). All cities are available as a point layer, but the largest ones are also available in the county layer. In these cases, the buffer is built around the city. A protection zone of 500 m is suitable for the building layer.

Protection zones of water bodies and roads have been established based on the Protection Zones Law

There is a 60 m lane on both sides of the centre line. This area also includes the width of the road itself. Individual road categories are not distinguished. According to the Law on Protection Zones, the streets correspond to the national, regional routes, an average class. There is a 50 m lane for railways.

Waterbody layer data is protected, making it challenging to calculate new value fields, but their area is not available in the standard data table. Consequently, a protection zone of 100 meters wide has been established for all water bodies, which according to the Law on Protection Zones, would correspond to water bodies of 25–100 hectares.

Watercourses are divided into categories, but it is not specified what these categories are. According to the data corresponding to the situation in nature, the most significant rivers have a higher class. Category 90 corresponds to the Daugava and the widest part of the Lielupe, a small part of the Venta and Gauja estuaries. A 400 m wide strip is allocated to this category (the entire length of the Daugava and the Gauja from Lejasciems to the mouth corresponds to 500 m, the Gauja from its source, the Lielupe and the Venta - 300 m). As large rivers at their widest points are also included in the aquifer layer, there are no places where the protection zone would be narrower than the river itself. Categories 60-80 have 300 m wide lanes corresponding to watercourses longer than 100 km. Categories 20-50 have 100 m wide streets corresponding to rivers longer than 25 km but shorter than 100 km. River lines of category 10 have a 50 m wide protection zone on each bank.

A 500 m buffer is used for the building layer.

Protected nature areas, significant nature objects, and areas over 200 m above sea level and with a slope steeper than 10% are excluded. The hill is not evaluated in detail since the overall geography of the country is close to 0-2.5 flat degrees. After that, areas that are smaller than 22 ha are excluded. The limit of 22 ha assumes that the turbine's rotor diameter will be

around 80 m based on the experience from the technical parameters in ongoing wind farm development projects. Each turbine needs 5x7 turbine diameters from another turbine.

Finally, narrow limitations such as rivers and roads are excluded from the available area. Still, they are not used as criteria for determining the fragmentation since it is possible to build turbines on two sides with the road and its protective buffer zone going in between.

Only an area closer than 3 km to the current energy grid is considered to reduce investment costs and energy loss. Therefore, the large available regions are considered the primary potential locations with a territory size of over 20 km^2. Table 3.3 provides an overview of the used parameters.

Table 3.3. Overview of the applied parameters [40].

Aspect	Parameter	Criteria	
Environmental	Slope	< 10 degrees	
	Land cover	protected nature area	
	Elevation	< 200 m	
Legislative and social	Protection zones	towns	> 2000 m
		villages	> 1000 m
		buildings	> 500 m
		waterbodies	> 100 m

The territory covered by the forest might be calculated separately since it is possible to install the turbines in the woods, and there could be such projects in future. However, there are currently no wind parks built in the forests in Latvia, and extra costs and lower efficiency in such areas must be considered.

The data obtained by GIS is used as an input in the SD model that estimates the future of the energy sector of Latvia through various political scenarios.

The new layers are grouped into one layer. The new single layer was cut using the contours of the planning regions.

3.1.4. Determination of excess heat potential

The possibility of integrating surplus heat is also analysed in the SD model. As the potential for excess heat is local, GIS modelling was used to determine the national potential.

In this study, a bottom-up approach is used, and the potential for excess heat is determined using the fuel consumption of the largest industrial enterprises (Figure 3.4). Fuel consumption reports of more than 200 companies are analysed by type of fuel and heat production technology. The amount of heat produced is calculated assuming a specific calorific value of combustion and efficiency factors of heat production technology for each fuel source (mainly natural gas and various wood biomass).
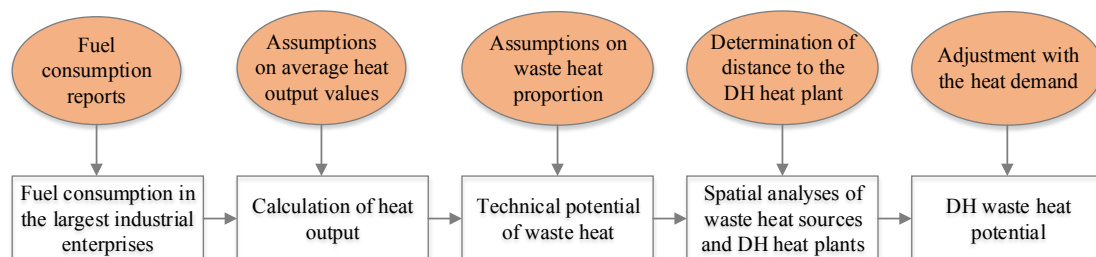

Fig. 3.4. Data acquisition methods

The results for the share of excess heat from previous studies have been used [42], [43]. Spatial analysis was used to define the technical surplus potential that could be integrated into DH systems. The identified sources of excess heat and the location of the DH heat stations are displayed on a background map in ArcGIS. DH heat plants' annual amount of heat production is determined using fuel consumption reports of DH companies and heat producers. The nearest DH heat boiler house has been selected for each industrial area with the potential for excess heat. The connection costs were determined for the analysed companies to assess the rationale for the integration of waste heat. The authors accept the average cost of DN80 pipelines as 300 EUR / m. The methodology described in the study [43] states that connection costs should not exceed 4.17 EUR / MWh / year delivered to the DH network.

Another aspect to consider is the available heat demand for surplus heat. Therefore, the obtained surplus heat potential must be related to the annual heat demand of a specific DH thermal power station. The authors identify the potential for surplus heat that exceeds the heat demand of a particular area, so the use of alternative heat should be considered.

The analysed industrial enterprises' total heat surplus potential is 272 GWh per year. The sources of surplus heat that should be integrated into the DH network have been identified using spatial analysis. Results of spatial analysis 3.5. The figure shows the distribution of industrial enterprises and DH boiler houses in the territory of Latvia. The map shows the heat energy demand (GWh / km2), the annual amount of surplus heat in the company (MWh per year) and the amount of heat produced in boiler houses (MWh per year).
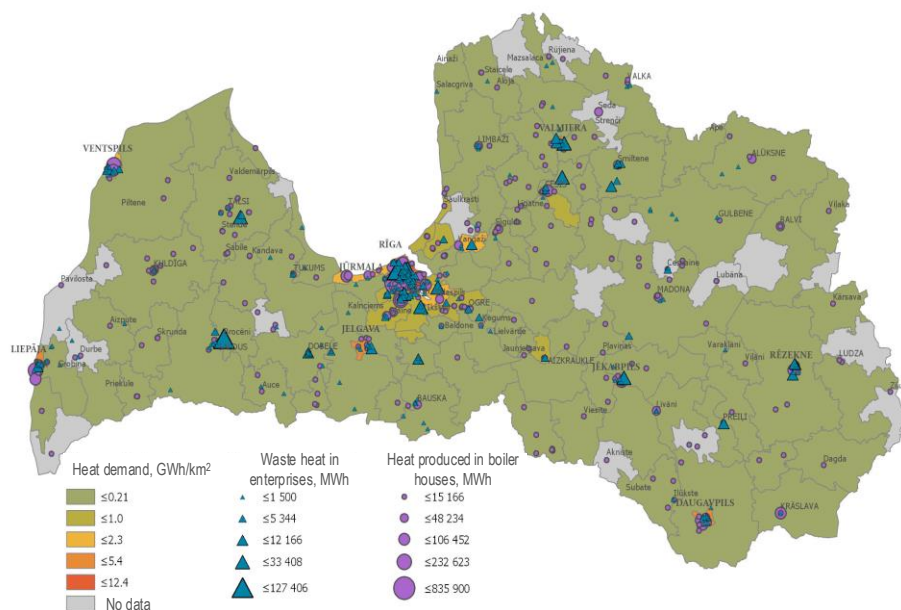

Fig.3.5. DH boiler houses and potential residual heat points

In the territory of Latvia, it is observed that the location of DH boiler houses is uneven. In some counties, boiler houses are located only in cities, and there are no DH boiler houses in the surrounding area. To determine industrial enterprises' technical and economic potential, the distance between the source of surplus heat and the nearest boiler house was determined. The distribution of companies by length to the nearest boiler house was used in the SD model.

3.2. Methodology for displaying SD model results in GIS structure

A visualisation tool has been developed to show shots of the SD model spatially. First, the GLS draft is designed to see if the data can be represented in a way that helps them be

understood. Created an HTML page with matching selection windows using standard CSS style sheets.

Use the slider to display the selected year in the tool, the drop-down for the other parameters. Listeners added to *JavaScript* code event to read output values.

The output files in the *.csv* file need to be translated for *JavaScript* to be read best. *Python* script used.

Data corresponding to the GLS selection uses an iteration cycle to replicate each file as an object with an annual parameter as the critical value.

The Leaflet base card is then added. To display the map in GLS, the polygons of the planning regions provided by Envirotech had to be translated from LKS 92 to EPSG: 3059. The file was saved as *.csv* and opened in *Excel*. An online tool is available at *https://epsg.io/* for quick conversions. A *Python* script was used to prepare the polygon file for conversion. After all, coordinates have been correctly displayed and recalculated using the *Excel* formula; the display format has been updated to match the parameters of the .geojson file. The file is saved as a regular *.js* file before adding the variable name to the data set to make it easier to replicate. Using an additional file. Model output files are translated into .js as well as *.csv* with model data.

Dynamic linking will be performed using the *BTPK_Py* library. The file extracted from the SD model is run in *.xmile* format via a custom *Python* script, thus obtaining most of the *STELLA* functionality in the form of code. Although the library is intended to transform the model as it currently stands directly, it only works with simpler models. As a result, several adjustments had to be made, for example, to detect if cycles in another cycle. You must also remove all Latvian diacritical marks made using *Python*. After obtaining the code, the input file is linked to a .js file containing information about the landfills' geography. Each polygon is assigned a model output value. The polygons are displayed in the user interface, where you can also select the model input parameters, which change the values in the code accordingly.

STELLA provides an application developer interface (API) to modify the standard model output interface. A card with marked polygons with the value of the markers corresponding to the output value is attached to the standard *STELLA* output. Given that *STELLA* displays all years simultaneously in the form of a graph, the user must select the year to be displayed on the map as an additional parameter.

3.3. Methodology for dynamic coupling of SD model with GIS

Further research will include the dynamic linkage of both models. In the case of wind energy, the merging of SD and GIS models will be continued by integrating the spatial differences regarding the distance from the transmission lines and average wind speeds in the particular territories.

For the convenience of sharing the results with stakeholders coupling the SD model with the GIS will be done in the web application. It will easily allow updates and is hassle-free for the end-users. Both SD and GIS models will be translated to the Python script, which works as stand-alone programs without a modelling environment. That will let to upload models to the webserver and create a web application to interact with these models using already well-established web frameworks.

For dynamic coupling, the SD model with GIS model, the web application can be used, mainly due to the benefits of the easy build of the graphical user interface, convenient way of sharing the results, and updates if necessary are hassle-free for users. The methodology for model dynamic linkage can be seen in Fig.3.6.
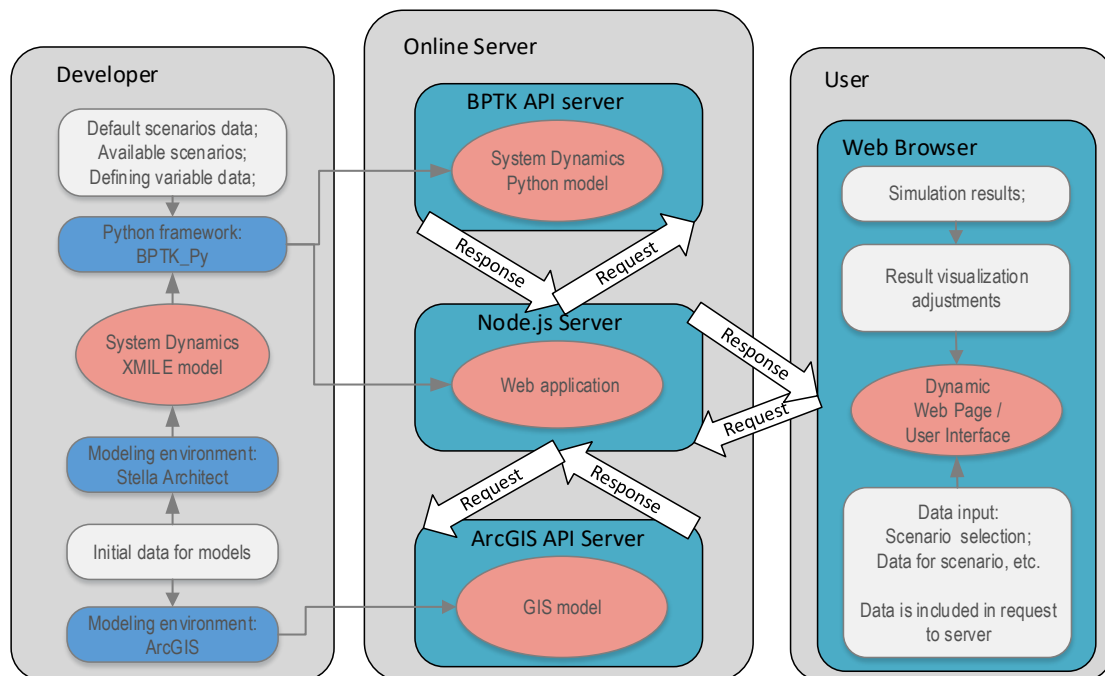

Fig.3.6. Dynamic linkage of developed models

Before coupling the models, creating both SD and GIS models is necessary. When both models are ready, they are translated into Python code that works as a stand-alone program without a modelling environment. That allows to upload these models to the webserver and create a web application to interact with these models by using already well-established web frameworks like Flask, React and Node.js.

To translate the SD model code into a python code, authors used BPTK_Py, a python framework developed by the German company "Transients"[1].

During the translation phase of the model, it is also necessary to define the possible scenarios that could be either predefined or static with already known variables, or it could also be defined as interactive scenarios

---

[1] https://www.transentis.com/business-prototyping-toolkit/en/

On the server, there are three programs, one for each model, that would be the so-called back-end servers and one for the user interface or front-end server. The front-end servers are waiting for the incoming data from the web page, which is coming in whenever a user makes changes in the web page, selects different scenarios, graphs, changes scenario data, visualisation of graphs.

When the Front-end server receives the data from the user, then it starts to send the information to one or both back end servers; that depends on what changes the user made in the web page. The request-response cycle between the servers/programs is provided via REST API. The front-end server uses the data gathered from the back-end servers to render the output file (HTML) that is read by the web browser and displays the requested results back to the user.

4. SPATIAL ANALYSES RESULTS

This section presents the results of the available RES spatial profile, the main primary energy sources used in different industries, the constraints on wind energy use in each region, and the results of the system dynamics model and visualisation tool.

4.1. Spatial analysis of available space and wind energy constraints

Regulations and restrictions related to the construction of wind farms pose a significant obstacle to the development of wind farms. This study analyses and adds the constraints on buffer zones around other infrastructure and natural sites to the SD model.

Figure 4.1. and 4.2. shows the intermediate results of the GIS analysis still in visual form. Figure 4.1. shows how the bounding layers overlap. In some cases, this could indicate places where restrictions could be lifted, such as if they are built around an uninhabited building that is still shown as inhabited. Figure 4.2. offers the final single layer.

Although the main result of the analysis is the total percentage that is not subject to any restrictions (Table 4.1), the map provides additional information, such as the fragmentation of the site. The distance to cities and the availability of electricity infrastructure can also be added to the resulting layer to assess the potential energy consumption and suitability of the site in terms of constraints and wind speeds and the practical potential for using local energy at the lowest possible cost.
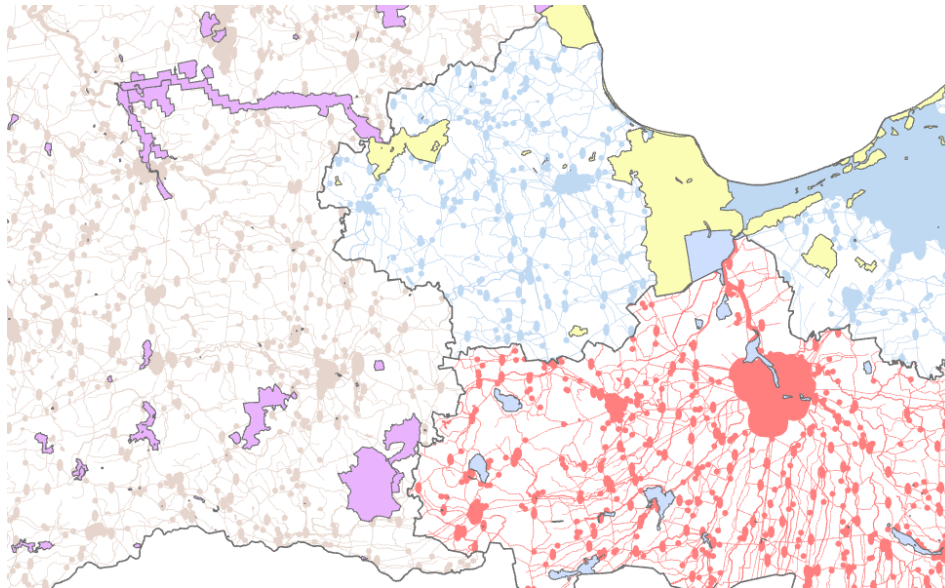

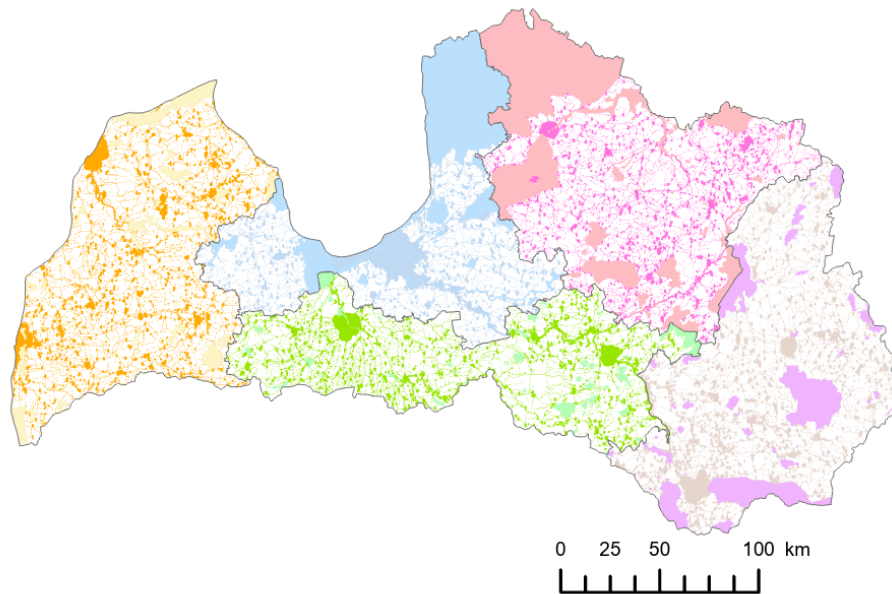Fig. 4.1. Fragment of restriction buffer zones

Fig. 4.2. Restrictions on the installation of wind turbines

The area available for installing wind turbines is approximately 70-80% of the total area. It should be noted that forests are included in the general area. There were no restrictions on nature parks and other protected areas. Given all this, the de facto open space is probably half that shown here.

The Merge function was used to make merging possible, which combined all layers as separate objects. The Dissolve tool then joined all the locations where several parameters overlapped into one layer but divided the individual things into areas that do not touch other objects that meet the constraint conditions. By repeating the *Merge* function, all objects are merged into one entity on one layer.

The area was calculated for the planning regions using the *Calculate* geometry function (Table 4.1). Using the *Split* process, the combined size of the unsuitable regions is divided into planning areas. The area of the new layer is calculated in each of them.

From the GIS model, the available land areas have been determined separately for the five planning regions of Latvia. As shown in Fig.4.3, the forests account for the largest excluded site in Kurzeme, Vidzeme, and Riga regions. However, these can be further considered in the simulation by applying different cost assumptions for installing wind farms in forests.

The results show that suitable wind farm installation is around 24% of the total land area in Latvia. However, within the Vidzeme and Latgale region, larger land areas are with geographical limitations due to higher territory slope.
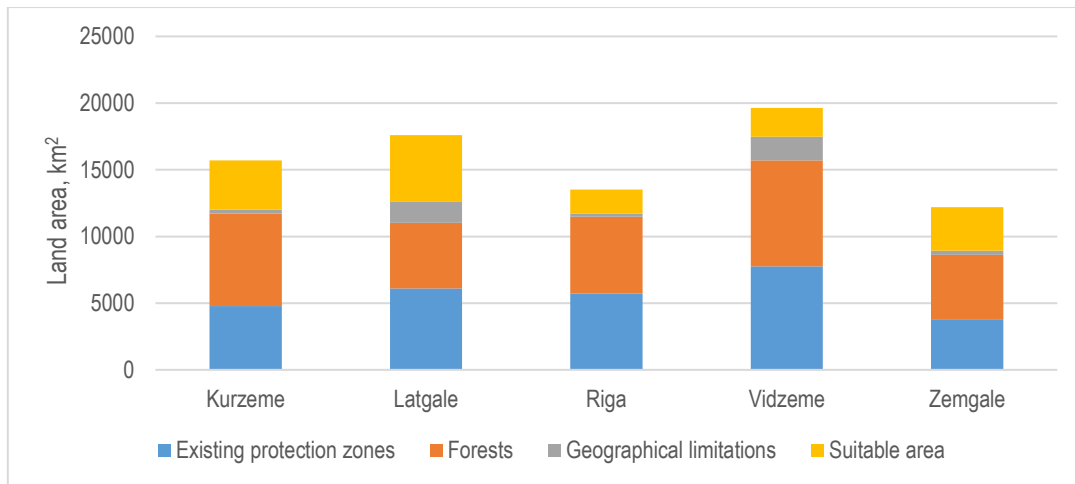
Fig.4.3. Land availability and excluded territories for each region

In addition, the GIS model allows evaluating the territories at a reasonable distance from the existing power grid (see Fig.4.4). Within the study, the GIS model excludes domains further than 3 km from the existing power grid by assuming that these territories would be economically beneficial without adding extra costs due to new transmission line installation. The results show that less than 30% of suitable land area would be in territories not too far from the transmission grid resulting in 4647 km^2 in Latvia. If typical wind turbines were installed, these territories could provide around 10.7 GW of power capacity.

In addition, small land territories are excluded by installing large wind parks, which could provide a higher share of RES and lower specific installation costs. When only environments larger than 20 km^2 are included, the total suitable land area is 2389 km^2 which could provide habitat for 5.5 GW of wind power.
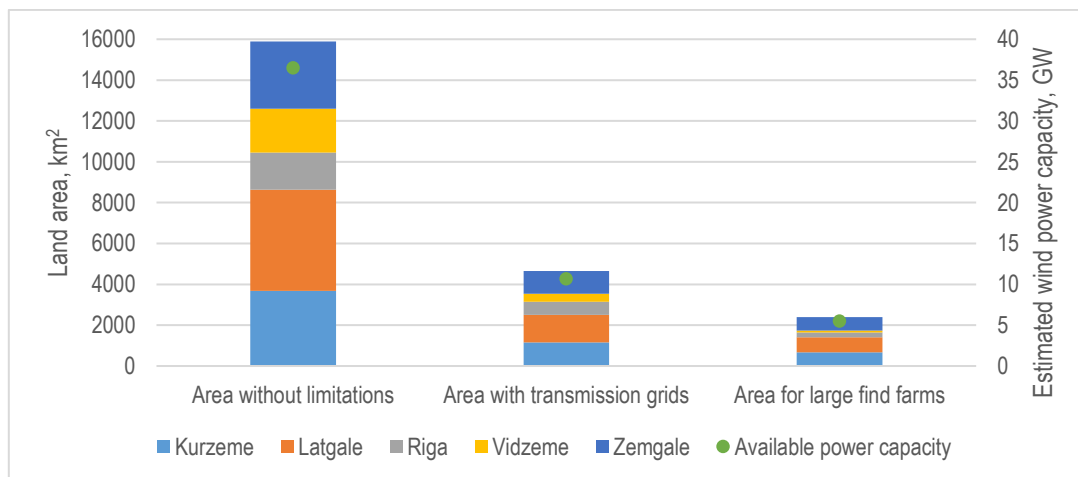
Fig.4.4. Comparison of available territories with transmission grids and suitable for large find farms

The results of spatial analyses are visualised in Fig.9, where the land areas with all spatial limitations are excluded (a) and additional restrictions when only the most extensive available land areas are marked (b). From the detailed maps, it can be seen that areas along the main power transmission grids are most suitable for wind park installation. However, only a few territories appropriate for large-scale wind park installation have been identified in the Vidzeme region as the land has a higher slope and smaller electricity transmission line density.

a)   b)
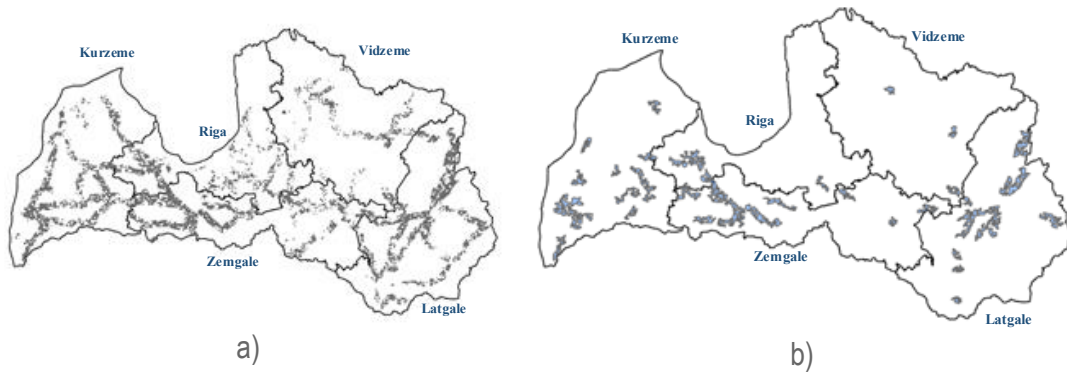
Fig. 4.5. Spatial analyses for all applied limitations (a) and the areas where large scale wind parks are possible (b)

The obtained results from GIS modelling have been included within the SD model to investigate further how the identified land areas would limit the reaching of RES power targets.

4.2. Data on household energy consumption

Household electricity consumption data are obtained using the bottom-up method. The obtained data are reconciled with the energy balance (Table 4.2).

Table 4.2

Energy consumption of households in the regions

Region	GWh
Kurzeme	218.76
Latgale	181.73
Riga	1059.17
Vidzeme	140.31
Zemgale	192.78

Although regional data are derived from the assumption, such data to the model provides additional information on provincial differences that cannot be obtained by dividing the energy balance result by population.
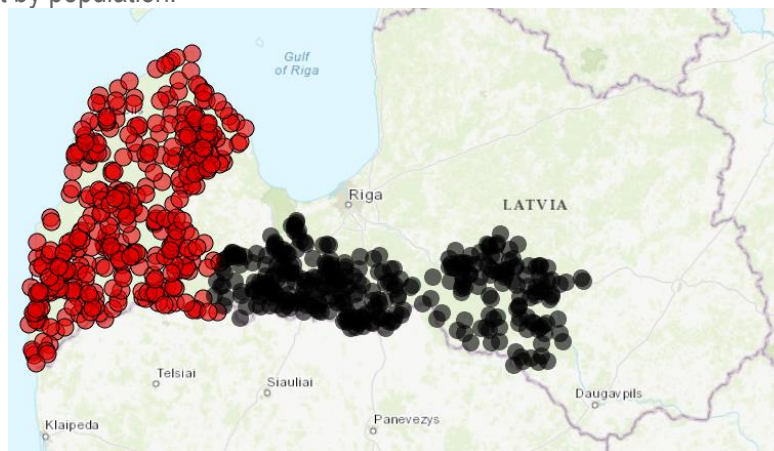
Fig. 4.6. Example of energy consumption data visualisation

Figure 4.6. shows the differences in household energy consumption data using the two methods. The first method estimates data differences based on available spatial information, taking into account all its limitations. The second distributes total consumption in proportion to the population. The difference is relatively small and could be considered insignificant if the focus of the study and the model were to analyse the overall energy consumption statistics. Here, given the aim of showing regional differences, even such distinctions are important.

As mentioned in the planning documents, the energy consumption of ZPR per capita is lower than the national average, and this can also be observed in Figure 4.7. However, the primary focus should be on the Latgale planning region, where per capita consumption is the lowest and may indicate a risk of energy poverty. Although reducing energy consumption is one of the goals of the climate, tackling social inequalities in the regions is also essential.
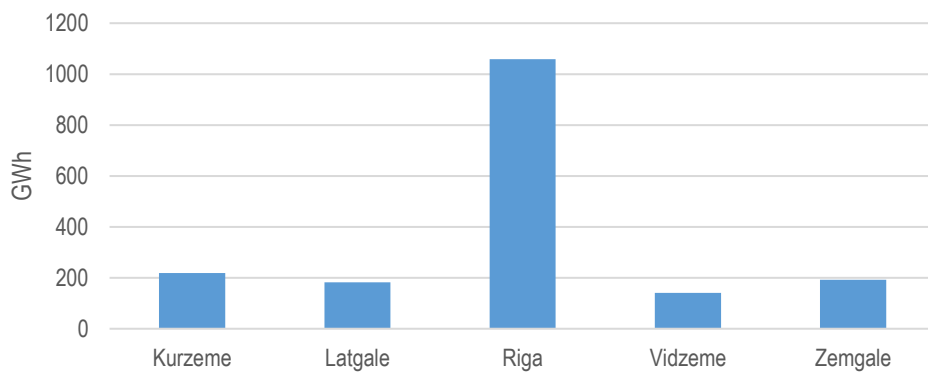
Fig. 4.7. Household energy consumption by region

4.3. Regional trends in the baseline scenario

The results of the SD model for the baseline scenario are discussed in the chapter in Figure 4.8. and 4.9. describes the energy produced by DH in the regions. Figure 4.5. shows the RPR. The differences in production are so significant that it is impossible to see trends in regions other than RPR. It would be helpful to look at Riga as a separate case and exclude it from the general regional observation, taking into account the level of urbanisation in Latvia and the concentration of population in the Riga conglomerate. However, in this case, excluding the whole RPR is not the best solution, as its rural areas are still more similar to the rest of Latvia than Riga. This will be possible in future studies if they focus on the municipal level. The decrease in the RPR of natural gas use will significantly affect the entire country, but it is essential to pay attention to the proportional reduction in gas consumption in Latgale.
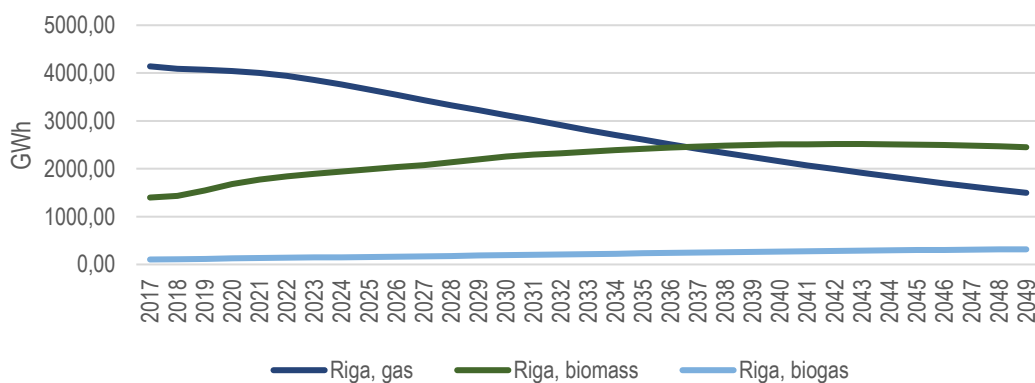
Fig. 4.8. Comparison of energy production trends in RPR
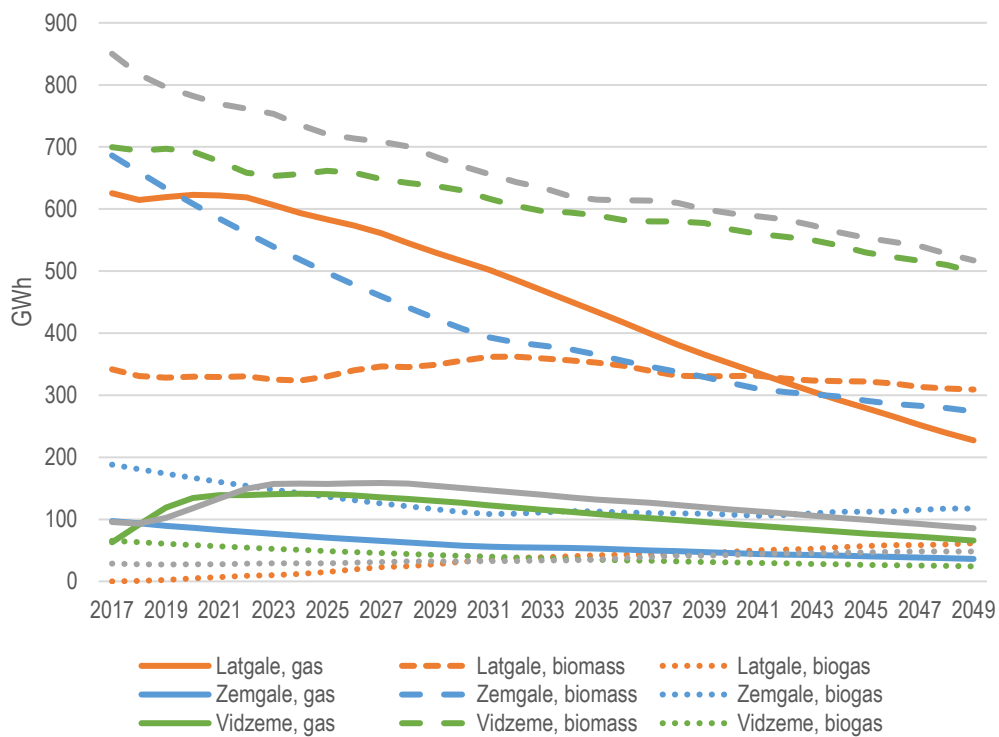
Fig. 4.9. Energy production KPR, LPR, VPR, ZPR

Looking at the changes in consumption in the Latgale planning region, significant positive trends can be observed, even if they are not so noticeable due to the smaller total amount. Figure 4.10. shows the trends in the share of RES in the region. The most dramatic changes are forecast for electricity generation, where a decline is expected at the beginning, followed by an increase.
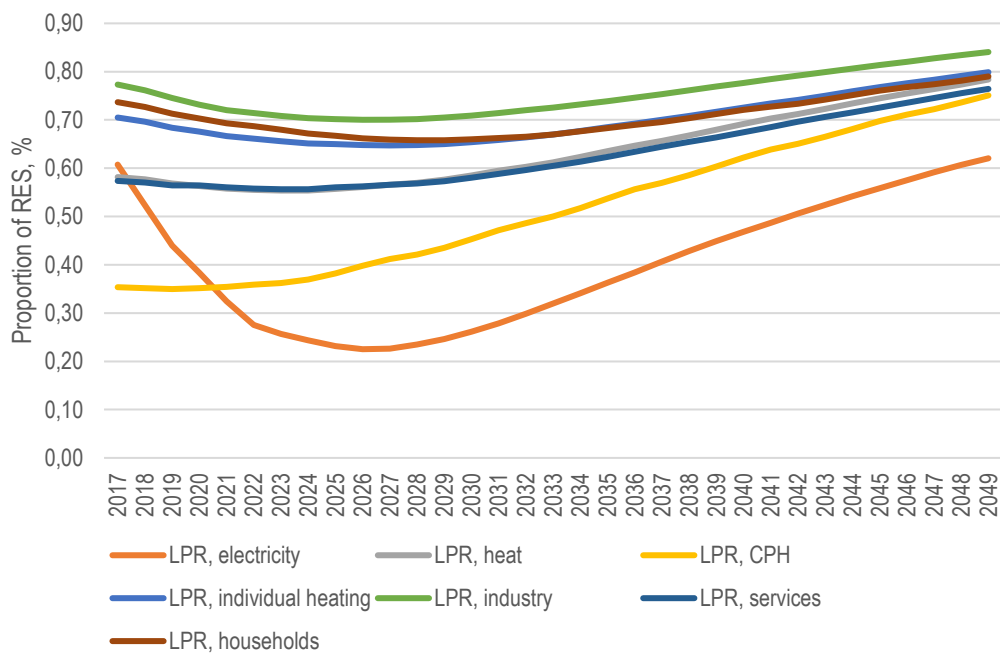
Fig. 4.10. RES share in LPR in all sectors

Comparing the other regional accounts, electricity generation is the section with the least stable forecasts, so Figure 4.11. compares this parameter in all planning regions. The only area where a decline is not expected before the subsequent increase is ZPR, where RES is already close to 100% due to electricity generation.
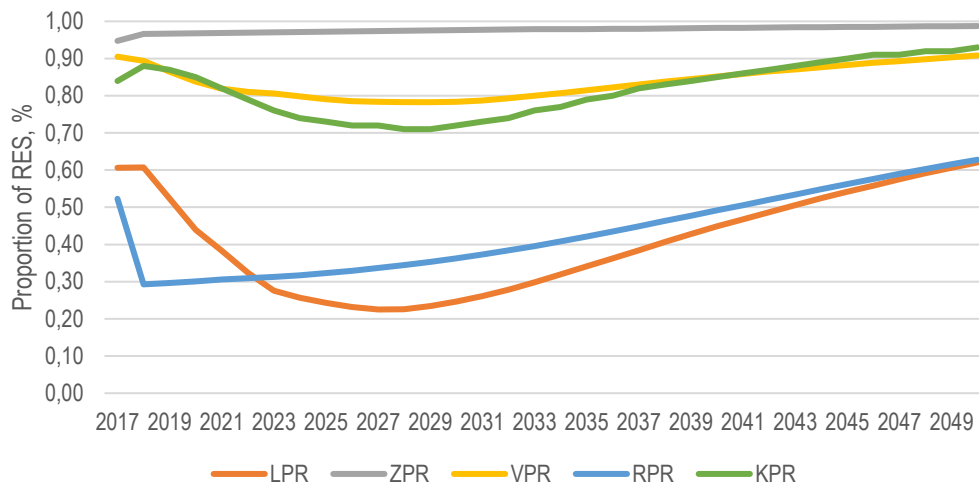
Fig.4.11. Comparison of RES share in electricity by regions

The obtained results from GIS modelling have been included within the SD model to investigate further how the identified land areas would limit the reaching of RES power targets.

The section presents the SD modelling results for two scenarios – Scenario 1 without support measures for wind park development and Scenario 2 with several policy instruments that could promote the rapid growth of wind farms in Latvia. Fig. 4.12 shows the overall national power production balances in each scenario. In Scenario 1, without additional support and promotion of wind energy, the total production rate increases from 120 GWh in 2020 to 437 GWh per year in 2050. However, a significant wind power increase has been observed when the support measures are included within the forecast. As a result, the total wind production rate will increase to 3760 GWh in 2050 by almost excluding natural gas from the consumed primary energy sources and reaching carbon-neutral power production. In this scenario also the imported power share decreases significantly.
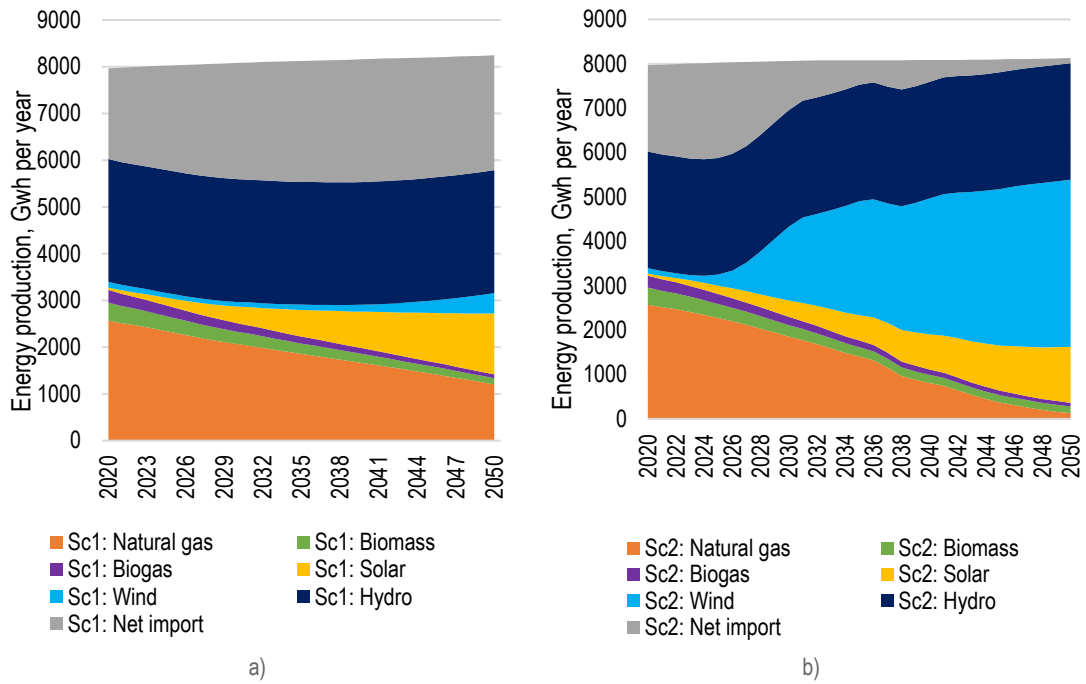
Fig.4.12. Comparison of energy source mix for power production in Scenario 1 (a) and Scenario (b)

The installed capacities of wind turbines in each scenario have been compared in Fig.4.13. The installed wind power capacity in Scenario 1 is 0.20 GW, but in Scenario 2, it reaches 1.55 GW. However, as shown in Fig. 4.13, only 28% of the identified potential from the land availability analyses reached 5.5 GW when applying all of the limiting criteria.
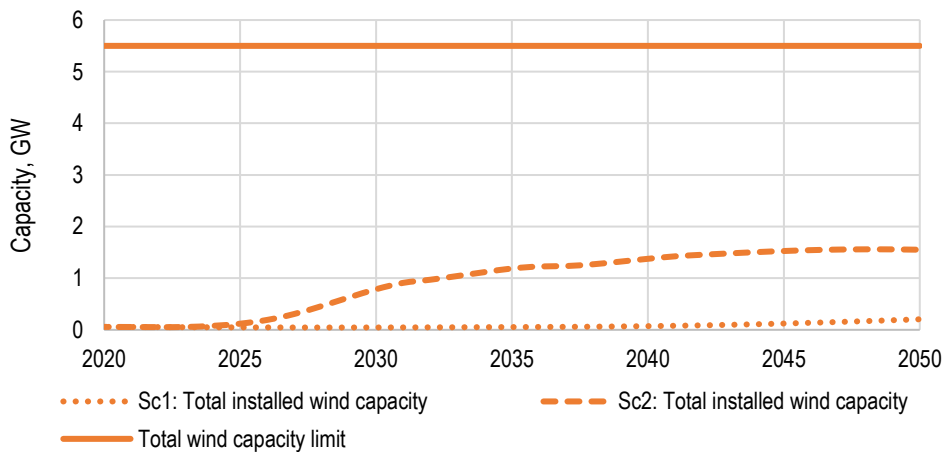
Fig.4.13. Comparison of installed wind power capacity in each scenario and the modelled limitation according to land availability

The modelled wind capacity has also been analysed within the spatial scale by considering the regional differences. The results for each region can be seen in Fig.4.14. The installed wind power capacities reach identified limitations for large-scale wind farms in the Vidzeme region. However, there could still be available territories for smaller-scale power parks and forest territories.
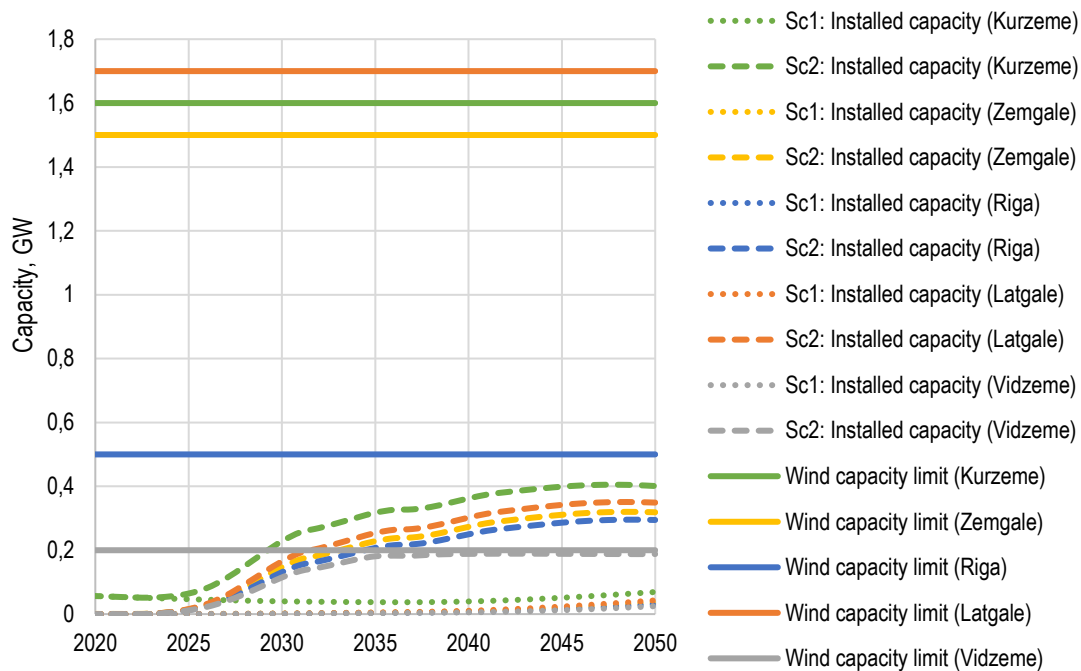
Fig.4.14. SD modelling results for each region

The GIS model's modelling results with integrated land availability limitations show enough appropriate territories for cost-effective onshore wind farm installations. The forecast indicates that the identified end of 5.5 GW could provide 8245 GWh of wind power per year, which is more than the forecasted total power consumption in Latvia in 2050 - 8129.5 GWh per year.

4.4. Visualization tool

Examples of RES development scenarios have been created to test the tool's operation. The tool uses the duplicate files for all three methods; however, it is fully ready to replace the files to accommodate the updated script files. The data described in this paper apply to the baseline scenario.

An interactive visualisation tool as shown in Figure 4.15. in the figure, allows the user to review the data easily. The user interface will enable you to select parameters and display the map's corresponding value. The current settings will enable you to choose the year, regardless of whether the technology is new or not, whether ETS quotas are applied, and the type of power plant.

Comparing the two images shows no indicative benefits of GLS. It offers less because only one year and parameter can be displayed at a time. However, there are secondary benefits, such as people tend to ignore extensive schedules. With the interactive component, it is possible to attract their attention to be an exciting addition to the project.

The cartographic approach to visualisation requires spatially diverse data.

The tool consists of 15 model output files. The data cover all five planning regions and three scenarios in each.

The tool has two active cursor positions, one of which marks the region, the other activates an additional information field and displays the unit of measure.
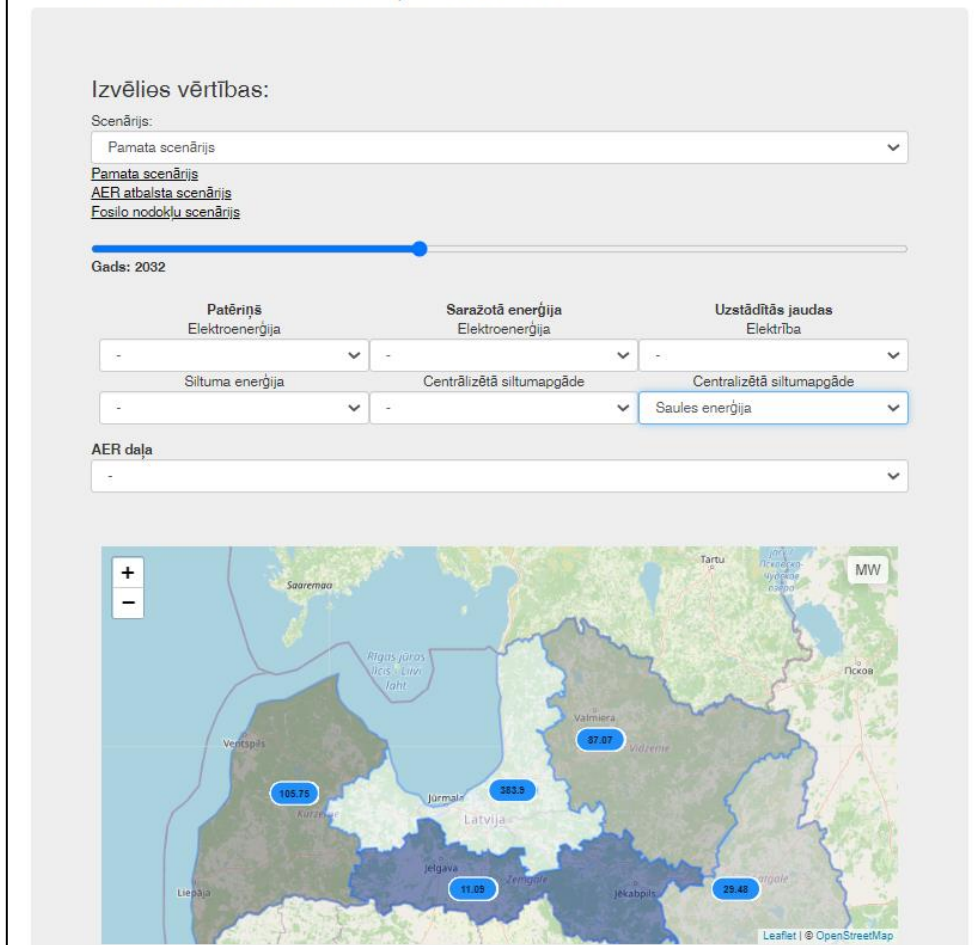
Fig.4.15. Visualisation tool interface

CONCLUSIONS AND RECOMMENDATIONS

According to the results of the analysis of regional data, most of the current energy produced and consumed from fossil fuels is RPR. The focus must be on replacing natural gas in the region. The resulting regional profiles can be used to input complex mathematical models in the energy sector.

KPR has a more significant potential for variable energy sources such as solar and wind and biomass. ZPR, meanwhile, has great potential for agricultural residues that could meet future energy demand. The possibility of the resources available for LPR and VPR is lower; however, these regions show a high share of RES in several sectors. Further research would be needed to improve cooperation between regions and municipalities to meet the growing demand for biomass and RES.

The obtained results show that spatial analyses are needed even in relatively small countries, such as Latvia, to identify obstacles to transforming the energy sector. Additional regional targets may need to be set, or the development of planning documents may need to be supported to avoid regional differences in the share of RES.

The research presents the methodology for soft linkage of GIS and SD models. Spatial modelling helps identify obstacles and limitations to the energy sector's transformation. The wind park installation has been analysed as a case study because land availability is an important limitation for this technology. However, further research could also have in-depth analyses for other resources, such as solar rooftop installations or available surplus heat integration for heat supply.

The obtained results show that when excluding the territories with environmental, legislative, and social limitations (high sole, forest areas, protected nature territories, towns, villages, water bodies etc.), the total land area appropriate for wind park installations decreases to 24% of total land area. In addition, there are also economic aspects that could increase or decrease the wind park installation costs, such as distance from the power grid and availability for large scale wind park installations. Therefore, the obtained limitation for cost-effective wind park installations is 2389.4 thousand km^2 which could provide 5.5 GW of wind power.

The obtained limitations have been integrated within the SD model to forecast the future development of the power sector. The results show that due to the high share of hydropower plants operating in Latvia, installing 1.55 GW of wind power is necessary to reach the climate-neutral power sector in 2050. Therefore, it can be concluded that there are enough land territories to provide such an amount of wind power. However, it is crucial to decrease the administrative barriers and provide information campaigns to reduce existing obstacles for onshore wind park installations in Latvia. Nevertheless, the existing policy planning documents focus on supporting offshore wind parks with higher installation costs than onshore wind parks.

The SD model also provides the analysis on a regional scale by analysing if there are appropriate territories for wind power development. Results show that only one region reaches the identified land availability limit, which indicates that a small amount of power will need to be transmitted from the other areas. However, the forecasted wind power capacities are far from the defined limit in 3 of 5 regions. Future research could also include the technical parameters of transmission lines by identifying the potential transmission capacities of the existing transmission infrastructure. However, there is no indication that new high voltage transmission lines would be necessary from the preliminary analyses.

Reference

[1] B. Resch *et al.*, "GIS-Based Planning and Modeling for Renewable Energy: Challenges and Future Research Avenues," *ISPRS Int. J. Geo-Information*, vol. 3, no. 2, pp. 662–692, May 2014, DOI: 10.3390/ijgi3020662.

[2] C. Spataru, *Whole energy system dynamics: Theory, modelling and policy*. Taylor and Francis Inc., 2017.

[3] M. F. Goodchild, "Chapter 1 ABSTRACT GIS and Modeling Overview," 2005.

[4] D. Sandor, S. Fulton, J. Engel-Cox, C. Peck, and S. Peterson, "System Dynamics of Polysilicon for Solar Photovoltaics: A Framework for Investigating the Energy Security of Renewable Energy Supply Chains," vol. 10, 2018.

[5] X. Liu, G. Mao, J. Ren, R. Y. M. Li, J. Guo, and L. Zhang, "How might China achieve its 2020 emissions target? A scenario analysis of energy consumption and CO2 emissions using the system dynamics model," *J. Clean. Prod.*, vol. 103, pp. 401–410, 2015, doi: https://doi.org/10.1016/j.jclepro.2014.12.080.

[6] P. C. Wingo, "OME: A Framework for Running Spatially Explicit System Dynamics Models," 2015.

[7] C. Neuwirth, A. Peck, and S. P. Simonović, "Modeling structural change in spatial system dynamics: A Daisyworld example," *Environ. Model. Softw.*, vol. 65, pp. 30–40, Mar. 2015, doi: 10.1016/j.envsoft.2014.11.026.

[8] A. Peck, C. Neuwirth, and S. P. Simonovic, "Water Resources Research Report Coupling System Dynamics with Geographic Information Systems: CCaR Project Report," 2014.

[9] L. Ieviņa, A. Vidžups, A. Blumberga, and D. Blumberga, "Mapping of Distributed Power Generation Versus Biomass Availability," in *2019 IEEE 60th International Scientific Conference on Power and Electrical Engineering of Riga Technical University (RTUCON)*, 2019, pp. 1–5, doi: 10.1109/RTUCON48111.2019.8982373.

[10] Z. Xu and V. Coors, "Combining system dynamics model, GIS and 3D visualization in sustainability assessment of urban residential development," *Build. Environ.*, vol. 47, no. 1, pp. 272–287, Jan. 2012, doi: 10.1016/j.buildenv.2011.07.012.

[11] P. Wingo, A. Brookes, and J. Bolte, "Modular and spatially explicit: A novel approach to system dynamics," *Environ. Model. Softw.*, vol. 94, pp. 48–62, Aug. 2017, doi: 10.1016/j.envsoft.2017.03.012.

[12] S. Gharib, "Synthesizing System Dynamics and Geographic Information Systems in a new method to Model and Simulate Environmental Systems," University of Bergen, 2008.

[13] J. Houghton, "PySD," 2015. https://github.com/JamesPHoughton/pysd/blob/master/docs/index.rst.

[14] D. Schroeck, "No Title," 2020. https://github.com/transentis/bptk_py_tutorial.

[15] O. Iannone, "Beginner's guide to Python in ArcGIS Pro, Part 1: Why?," 2019. https://www.esri.com/arcgis-blog/products/arcgis-pro/uncategorized/beginners-guide-to-python-in-arcgis-pro-part-1-why/.

[16] ArcGIS Pro, "ArcGIS Pro Python reference."

[17] B. Naimi, "No Title." http://www.r-gis.net/stellar/.

[18] "Reģionālās attīstības likums," *Latv. Vēstnesis*, vol. 53, 2002.

[19] VARAM, "Kurzemes plānošanas reģiona Ilgtspējīgas attīstības stratēģija," 2015.

[20] Latgales plānošanas reģions, "Enerģijas datu pieejamības veicināšana 5 Latgales plānošanas reģiona pašvaldībās." http://www.lvif.gov.lv/?object_id=30652.

[21] VARAM, Rīgas plānošanas reģions, and N. Grants, "Rīgas plānošanas reģiona pašreizējās situācijas raksturojums un analīze."

[22] Ekodoma and Rīgas plānošanas reģions, "Rīgas plānošanas reģiona siltumapgādes attīstības rīcības programma," 2016.

[23] Vidzemes plānošanas reģions, "Reģionālais profils energoapgādes, patēriņa un energopārvaldības jomā," 2018.

[24] Zemgales plānošanas reģions, "Zemgales plānošanas reģiona Enerģētikas rīcības plāns 2018-2025," 2018.

[25] M. Kacare, I. Pakere, A. Grāvelsiņš, and D. Blumberga, "Spatial analysis of renewable energy sources," 2021.

[26] Ekonomikas ministrija, "Enerģētikas stratēģija 2030," 2011.

[27] M. Mohammadi and I. Harjunkoski, "Performance analysis of waste-to-energy technologies for sustainable energy generation in integrated supply chains," *Comput. Chem. Eng.*, vol. 140, p. 106905, Sep. 2020, doi: 10.1016/j.compchemeng.2020.106905.

[28] Technical University of Denmark, "Global Wind Atlas." https://www.globalwindatlas.info/.

[29] European Commission Joint Research Centre, "Photovoltaic Geographical Information System (PVGIS) | EU Science Hub," 2020. .

[30] LVĢMC, "2 Ūdens kopsavilkumi," 2019. .

[31] Lauksaimniecības datu centrs, "Dzīvnieku skaita statistika," 2020. .

[32] Latvijas Republikas Zemkopības Ministrija, "Latvijas Republikas Zemkopības ministrija Uzņēmumu tehniskie noteikumi (nozares standarts)," 2008.

[33] Lauku atbalsta dienests, "Deklarēto kultūraugu platību apjoms pa novadiem un pagastiem par 2018. gadu," 2018.

[34] Centrālā statistikas pārvalde, "Lauksaimniecības kultūru sējumu platība, kopraža un vidējā ražība," 2020. .

[35] S. Rozakis, D. Kremmydas, R. Pudełko, M. Borzecka-Walker, and A. Faber, "Straw potential for energy purposes in Poland and optimal allocation to major co-firing power plants," *Biomass and Bioenergy*, vol. 58, pp. 275–285, Nov. 2013, doi: 10.1016/j.biombioe.2013.06.011.

[36] N. Kara, "Yield and Mineral Nutrition Content of Buckwheat (Fagopyrum esculentum Moench): The Effect of Harvest Times," *Süleyman Demirel Üniversitesi Ziraat fakültesi Derg.*, vol. 9, no. 1, pp. 85–94, Mar. 2014.

[37] European Communities, "Cereals Straw Resources for bioenergy in the European Union," Luxembourg, 2007.

[38] Valsts meža dienests, "Meža statistikas CD," 2019. https://www.zm.gov.lv/valsts-meza-dienests/statiskas-lapas/publikacijas-un-statistika/meza-statistikas-cd?nid=1809#jump.

[39] P. Townsend, *Forest Biomass of Living, Merchantable Trees in Nova Scotia*. Nova Scotia Department of Natural Resources, 2008.

[40] Saeima, "Aizsargjoslu likums," *Latv. Vēstnesis*, vol. 56/57, 1997, [Online]. Available: https://likumi.lv/ta/id/42348-aizsargjoslu-likums.

[41] Latvijas Vēstnesis, *Aizsargjoslu likums*. Latvija, 1997.

[42] G. P. Panayiotou *et al.*, "Preliminary assessment of waste heat potential in major European industries," in *Energy Procedia*, Sep. 2017, vol. 123, pp. 335–345, doi: 10.1016/j.egypro.2017.07.263.

[43] F. Bühler, S. Petrović, K. Karlsson, and B. Elmegaard, "Industrial excess heat for district heating in Denmark," *Appl. Energy*, vol. 205, pp. 991–1001, Nov. 2017, doi: 10.1016/j.apenergy.2017.08.032.

ANNEX 1

HTML code of visualization tool

```
1.        <!DOCTYPE html>
2.        <html lang="en">
3.         <head>
4.          <title>SD model output</title>
5.          <link                                              rel="stylesheet"
href="https://maxcdn.bootstrapcdn.com/bootstrap/3.3.7/css/bootstrap.min.css"
integrity="sha384-
BVYiiSIFeK1dGmJRAkycuHAHRg32OmUcww7on3RYdg4Va+PmSTsz/K68vbdEjh4u"
crossorigin="anonymous">
6.          <link     rel="stylesheet"     href="https://unpkg.com/leaflet@1.7.1/dist/leaflet.css"
integrity="sha512-
xodZBNTC5n17Xt2atTPuE1HxjVMSvLVW9ocqUKLsCC5CXdbqCmblAshOMAS6/keqq/sMZ
MZ19scR4PsZChSR7A==" crossorigin=""/>
7.          <script              src="https://cdnjs.cloudflare.com/ajax/libs/leaflet/1.7.1/leaflet.js"
crossorigin=""></script>
8.          <link rel="stylesheet" href="style.css">
9.         </head>
10.
11.        <body onload="model">
12.         <div class="container">
13.          <h1>SD model output</h1>
14.          <div class="jumbotron">
15.          <h3>Choose values:</h3>
16.        <div class="form-group">
17.
18.        <div>
19.        Scenario:
20.            <select class="form-control" id="scenario">
21.             <option value="1">The baseline scenario</option>
22.             <option value="2">Fossil fuel tax scenario</option>
23.             <option value="3">Renewable energy support scenario </option>
24.            </select>
25.        </div>
26.
27.        <a href=" " title="Considers the development of the heating system without the use
of policy instruments is assessed. Excise duty is maintained at the level of 2017, as the
legislation does not currently foresee and approve an increase in excise duty. The natural
resources tax on the emitted CO2 emissions is increasing by 2022 in line with the values
approved by the legislation, and after 2022 it is no longer increased. The amount of support
granted for promoting energy efficiency and approved by 2020 shall be allocated and used by
2023. Once the current funds have been used, no new funding for energy efficiency will be
allocated. No financial support is granted for the integration of RES, replacement of DH system
networks, and for the transition to low-temperature heating." style="color:#000000;text-
decoration:underline">The baseline scenario</a>
28.        <br>
29.          <a href=" " title="Excise duty on natural gas and natural resource tax on CO2
emissions is increased. The excise duty on natural gas approved in Latvia is 1.65 EUR per
```

MWh for fuel use in heat supply. The excise duty is increased by 8 % per annum to around 22.5 EUR per MWh in 2050.The Natural Resources Tax (NRT) was 4.5 EUR per tCO2 in 2020. The legislative acts have approved the increase of rates to 15 EUR per tCO2 in 2022. For the emission trading system (ETS) installations, emissions costs are determined by the price of emission allowances. The NRT does not apply to the household sector. In the fossil fuel tax scenario, the NRT gradually rises to the ETS quota price level after 2022. The ETS quota price is adopted based on recommendations from the European Commission, which forecasts an increase in the quota price to around 50 EUR per 1 quota in 2040." style="color:#000000;text-decoration:underline">Fossil fuel tax scenario

30.
31.   Renewable energy support scenario
32.

33.   <div class="slider">
34.   <input type="range" min="2020" max="2050" onchange="f1(this.value)" value="1" class="slider" id="range">
35.   <label>Year: </label>
36.   </div>
37.
38.   <div class="form-group">
39.   <table border=0 >
40.   <tr><td colspan=3>
41.   <td width=210pt>
42.   <center>Consumption

43.   Electricity
44.   <select class="form-control" id="sector_e">
45.   <option selected="def">-</option>
46.   <option value="EPrupn">Industry</option>
47.   <option value="EPpak">Services</option>
48.   <option value="EPpub">Public</option>
49.   <option value="EPmaj">Households</option>
50.   <option value="EPkop">Total</option>
51.   </select>
52.   Heat
53.   <select class="form-control" id="sector_h">
54.   <option selected="def">-</option>
55.   <option value="SPrupn">Industry</option>

```
56.            <option value="SPpak">Services</option>
57.            <option value="SPpub">Public</option>
58.            <option value="SPmaj">Households</option>
59.            <option value="SPkop">Total</option>
60.          </select>
61.        </td>
62.        <td  width=33%>
63.         <center><b>Produced energy<br></b>
64.         Electricity
65.         <select class="form-control" id="res_e_p">
66.          <option selected="def">-</option>
67.          <option value="PRel[DG]">Natural gas</option>
68.          <option value="PRel[BM]">Biomass</option>
69.          <option value="PRel[BG]">Biogas</option>
70.          <option value="PRel[FR]">Fossil Fuel</option>
71.         </select>
72.         District heating
73.         <select class="form-control" id="res_h_p">
74.          <option selected="def">-</option>s
75.          <option value="PRDH[DG]">Natural gas</option>
76.          <option value="PRDH[BM]">Biomass</option>
77.          <option value="PRDH[BG]">Biogas</option>
78.          <option value="PRDH[FR]">Fossil Fuel</option>
79.         </select>
80.        </td>
81.        <td  width=33%>
82.         <center><b>Installed capacities<br></b>
83.         Electricity
84.         <select class="form-control" id="res_e_c">
85.          <option selected="def">-</option>
86.          <option value="ELcap[DG]">Natural gas</option>
87.          <option value="ELcap[BM]">Biomass</option>
88.          <option value="ELcap[BG]">Biogas</option>
89.          <option value="ELcap[S]">Solar</option>
90.          <option value="ELcap[V]">Wind</option>
91.          <option value="ELcap[H]">Hydro</option>
92.         </select>
93.         District heating
94.         <select class="form-control" id="res_h_c">
95.          <option selected="def">-</option>
96.          <option value="DHcap[DG]">Natural gas</option>
97.          <option value="DHcap[BM]">Biomass</option>
98.          <option value="DHcap[BG]">Biogas</option>
99.          <option value="DHcap[S]">Solar</option>
100.          <option value="DHcap[SS]">Heat pump</option>
101.          <option value="DHcap[PS]">Residual heat</option>
102.         </select>
103.        </td>
104.       </table>
105.      </div>
```

```html
106.        <div>
107.         <center><b>RES share</b>
108.          <select class="form-control" id="share" width=50pt>
109.            <option selected="def">-</option>
110.            <option value="AERel">Electricity production</option>
111.            <option value="AERsiltKop">Heating systems, total</option>
112.            <option value="AERsiltDH">District heating</option>
113.            <option value="AERsiltindiv">Individual heating systems</option>
114.            <option value="AERrupn">Industry</option>
115.            <option value="AERpakpub">Public</option>
116.            <option value="AERmaj">Households</option>
117.          </select>
118.        </div>
119.        </div>
120.      <br><br>
121.      <div id="map" style="width: 800px; height: 400px;" class="center-fit"></div>
122.
123.       <script src="modelKurzeme1.js"></script>
124.       <script src="modelLatgale1.js"></script>
125.       <script src="modelZemgale1.js"></script>
126.       <script src="modelRiga1.js"></script>
127.       <script src="modelVidzeme1.js"></script>
128.       <script src="modelKurzeme2.js"></script>
129.       <script src="modelLatgale2.js"></script>
130.       <script src="modelZemgale2.js"></script>
131.       <script src="modelRiga2.js"></script>
132.       <script src="modelVidzeme2.js"></script>
133.       <script src="modelKurzeme3.js"></script>
134.       <script src="modelLatgale3.js"></script>
135.       <script src="modelZemgale3.js"></script>
136.       <script src="modelRiga3.js"></script>
137.       <script src="modelVidzeme3.js"></script>
138.       <script src="main.js"></script>
139.     </body>
140.   </html>
141.
```

```
1.      var slider = document.getElementById("range");
2.      var output = document.getElementById("year");
3.      output.innerHTML = slider.value;
4.
5.      var sector_e = document.getElementById("sector_e");
6.      var sector_h = document.getElementById("sector_h");
7.      var res_e_p = document.getElementById("res_e_p");
8.      var res_h_p = document.getElementById("res_h_p");
9.      var res_e_c = document.getElementById("res_e_c");
10.     var res_h_c = document.getElementById("res_h_c");
11.     var share = document.getElementById("share");
12.
13.     var v = 0;
14.     var l = 0;
15.     var k = 0;
16.     var z = 0;
17.     var r = 0;
18.     var u = "-";
19.
20.
21.     var geojson;
22.
23.     var regions = [{
24.       "type": "Feature",
25.       "properties": {"reg": "Vidzeme Planning Region","val": v},
26.       "geometry":{
27.         "type":"Polygon",
28.         "coordinates":[[
29.     ...
30.         [27.6905697687,57.3700111292],
31.         [27.6737791733,57.3938946617],
32.         [27.6239465448,57.4017700711],
33.
34.     ...             ]]}
35.       }];
36.
37.     scenario.addEventListener('change', function () {
38.       scenario.value = this.value;
39.       map.removeLayer(geojson)
40.       upd();
41.       });
42.
43.     slider.oninput = function f1() {
44.       slider.value = this.value;
45.       output.innerHTML = this.value;
46.       map.removeLayer(geojson)
47.       upd();
48.     };
```

```
49.
50.     sector_e.addEventListener('change', function () {
51.         sector_e.value = this.value;
52.         document.getElementById("sector_h").value = "-";
53.         document.getElementById("res_e_p").value = "-";
54.         document.getElementById("res_h_p").value = "-";
55.         document.getElementById("res_e_c").value = "-";
56.         document.getElementById("res_h_c").value = "-";
57.         document.getElementById("share").value = "-";
58.         u = "GWh/y";
59.         map.removeLayer(geojson)
60.         upd();
61.     });
62.
63.     sector_h.addEventListener('change', function () {
64.         sector_h.value = this.value;
65.         document.getElementById("sector_e").value = "-";
66.         document.getElementById("res_e_p").value = "-";
67.         document.getElementById("res_h_p").value = "-";
68.         document.getElementById("res_e_c").value = "-";
69.         document.getElementById("res_h_c").value = "-";
70.         document.getElementById("share").value = "-";
71.         u = "GWh/y";
72.         map.removeLayer(geojson)
73.         upd();
74.     });
75.
76.     res_e_p.addEventListener('change', function () {
77.         res_e_p.value = this.value;
78.         document.getElementById("sector_e").value = "-";
79.         document.getElementById("sector_h").value = "-";
80.         document.getElementById("res_h_p").value = "-";
81.         document.getElementById("res_e_c").value = "-";
82.         document.getElementById("res_h_c").value = "-";
83.         document.getElementById("share").value = "-";
84.         u = "GWh/y";
85.         map.removeLayer(geojson)
86.         upd();
87.     });
88.
89.     res_h_p.addEventListener('change', function () {
90.         res_h_p.value = this.value;
91.         document.getElementById("sector_e").value = "-";
92.         document.getElementById("sector_h").value = "-";
93.         document.getElementById("res_e_p").value = "-";
94.         document.getElementById("res_e_c").value = "-";
95.         document.getElementById("res_h_c").value = "-";
96.         document.getElementById("share").value = "-";
97.         u = "GWh/y";
98.         map.removeLayer(geojson)
```

```
99.        upd();
100.
101.     });
102.
103.     res_e_c.addEventListener('change', function () {
104.        res_e_c.value = this.value;
105.        document.getElementById("sector_e").value = "-";
106.        document.getElementById("sector_h").value = "-";
107.        document.getElementById("res_e_p").value = "-";
108.        document.getElementById("res_h_p").value = "-";
109.        document.getElementById("res_h_c").value = "-";
110.        document.getElementById("share").value = "-";
111.        u = "MW";
112.        map.removeLayer(geojson)
113.        upd();
114.     });
115.     res_h_c.addEventListener('change', function () {
116.        res_h_c.value = this.value;
117.        document.getElementById("sector_e").value = "-";
118.        document.getElementById("sector_h").value = "-";
119.        document.getElementById("res_e_p").value = "-";
120.        document.getElementById("res_h_p").value = "-";
121.        document.getElementById("res_e_c").value = "-";
122.        document.getElementById("share").value = "-";
123.        u = "MW";
124.        map.removeLayer(geojson)
125.        upd();
126.     });
127.
128.     share.addEventListener('change', function () {
129.        share.value = this.value;
130.        document.getElementById("sector_e").value = "-";
131.        document.getElementById("sector_h").value = "-";
132.        document.getElementById("res_e_p").value = "-";
133.        document.getElementById("res_h_p").value = "-";
134.        document.getElementById("res_e_c").value = "-";
135.        document.getElementById("res_h_c").value = "-";
136.        u = "-";
137.        map.removeLayer(geojson)
138.        upd();
139.     });
140.
141.     var map = L.map('map').setView([56.88, 24.60], 7);
142.
143.     L.tileLayer('https://{s}.tile.openstreetmap.org/{z}/{x}/{y}.png', {
144.        attribution:                    '©                    <a
href="https://www.openstreetmap.org/copyright">OpenStreetMap</a>'
145.     }).addTo(map);
146.
147.     function label() {
```

```
148.        mv  =  L.marker([57.2,  26]).bindTooltip(v.toString(),  {  permanent:  true,
className:"label" }).addTo(map).setOpacity(0);
149.        ml = L.marker([56.3, 27.5]).bindTooltip(l.toString(), { permanent: true, className:
"label" }).addTo(map).setOpacity(0);
150.        mz  =  L.marker([56.3,  24.60]).bindTooltip(z.toString(),  {  permanent:  true,
className: "label" }).addTo(map).setOpacity(0);
151.        mk  =  L.marker([56.88,  21.6]).bindTooltip(k.toString(),  {  permanent:  true,
className: "label" }).addTo(map).setOpacity(0);
152.        mr = L.marker([56.9, 24]).bindTooltip(r.toString(), { permanent: true, className:
"label" }).addTo(map).setOpacity(0);
153.    };
154.
155.    label()
156.
157.    function upd() {
158.       if (scenario.value=="1") {
159.          var dataKurzeme = dataKurzeme1;
160.          var dataLatgale = dataLatgale1;
161.          var dataRiga = dataRiga1;
162.          var dataVidzeme = dataVidzeme1;
163.          var dataZemgale = dataZemgale1;
164.       } else if (scenario.value=="2") {
165.          var dataKurzeme = dataKurzeme2;
166.          var dataLatgale = dataLatgale2;
167.          var dataRiga = dataRiga2;
168.          var dataVidzeme = dataVidzeme2;
169.          var dataZemgale = dataZemgale2;
170.       } else if (scenario.value=="3") {
171.          var dataKurzeme = dataKurzeme3;
172.          var dataLatgale = dataLatgale3;
173.          var dataRiga = dataRiga3;
174.          var dataVidzeme = dataVidzeme3;
175.          var dataZemgale = dataZemgale3;
176.       }
177.
178.
179.       function find(array, key, value){
180.          for (var i = 0; i < array.length; i++) {
181.             if (array[i][key] == value) {
182.                if (sector_e.value=="EPrupn") {
183.                   return array[i][sector_e.value];
184.                };
185.
186.                if (sector_e.value=="EPpak") {
187.                   return array[i][sector_e.value];
188.                } else if (sector_e.value=="EPpub") {
189.                   return array[i][sector_e.value];
190.                } else if (sector_e.value=="EPmaj") {
191.                   return array[i][sector_e.value];
192.                } else if (sector_e.value=="EPkop") {
```

```
193.               return array[i][sector_e.value];
194.
195.            };  if (sector_h.value=="SPrupn") {
196.               return array[i][sector_h.value];
197.            } else if (sector_h.value=="SPpak") {
198.               return array[i][sector_h.value];
199.            } else if (sector_h.value=="SPpub") {
200.               return array[i][sector_h.value];
201.            } else if (sector_h.value=="SPmaj") {
202.               return array[i][sector_h.value];
203.            } else if (sector_h.value=="SPkop") {
204.               return array[i][sector_h.value];
205.
206.            } else if (res_e_p.value=="PRel[DG]") {
207.               return array[i][res_e_p.value];
208.            } else if (res_e_p.value=="PRel[BM]") {
209.               return array[i][res_e_p.value];
210.            } else if (res_e_p.value=="PRel[BG]") {
211.               return array[i][res_e_p.value];
212.            } else if (res_e_p.value=="PRel[A]") {
213.               return array[i][res_e_p.value];
214.            } else if (res_e_p.value=="PRel[FR]") {
215.               return array[i][res_e_p.value];
216.
217.            } else if (res_h_p.value=="PRDH[DG]") {
218.               return array[i][res_h_p.value];
219.            } else if (res_h_p.value=="PRDH[BM]") {
220.               return array[i][res_h_p.value];
221.            } else if (res_h_p.value=="PRDH[BG]") {
222.                return array[i][res_h_p.value];
223.            } else if (res_h_p.value=="PRDH[A]") {
224.               return array[i][res_h_p.value];
225.            } else if (res_h_p.value=="PRDH[FR]") {
226.               return array[i][res_h_p.value];
227.
228.            } else if (res_e_c.value=="ELcap[DG]") {
229.               return array[i][res_e_c.value];
230.            } else if (res_e_c.value=="ELcap[BM]") {
231.               return array[i][res_e_c.value];
232.            } else if (res_e_c.value=="ELcap[BG]") {
233.               return array[i][res_e_c.value];
234.            } else if (res_e_c.value=="ELcap[S]") {
235.               return array[i][res_e_c.value];
236.            } else if (res_e_c.value=="ELcap[V]") {
237.               return array[i][res_e_c.value];
238.            } else if (res_e_c.value=="ELcap[H]") {
239.               return array[i][res_e_c.value];
240.
241.            } else if (res_h_c.value=="DHcap[DG]") {
242.               return array[i][res_h_c.value];
```

```
243.            } else if (res_h_c.value=="DHcap[BM]") {
244.                return array[i][res_h_c.value];
245.            } else if (res_h_c.value=="DHcap[BG]") {
246.                return array[i][res_h_c.value];
247.            } else if (res_h_c.value=="DHcap[S]") {
248.                return array[i][res_h_c.value];
249.            } else if (res_h_c.value=="DHcap[SS]") {
250.                return array[i][res_h_c.value];
251.            } else if (res_h_c.value=="DHcap[PS]") {
252.                return array[i][res_h_c.value];
253.
254.            } else if (share.value=="AERel") {
255.                return array[i][share.value];
256.            } else if (share.value=="AERsiltKop") {
257.                return array[i][share.value];
258.            } else if (share.value=="AERsiltDH") {
259.                return array[i][share.value];
260.            } else if (share.value=="AERsiltindiv") {
261.                return array[i][share.value];
262.            } else if (share.value=="AERrupn") {
263.                return array[i][share.value];
264.            } else if (share.value=="AERpakpub") {
265.                return array[i][share.value];
266.            } else if (share.value=="AERmaj") {
267.                return array[i][share.value];
268.            }
269.         }
270.       }
271.     }
272.
273.    v = Math.round(find(dataVidzeme, "Years", slider.value) * 100) / 100 ;
274.    l = Math.round(find(dataLatgale, "Years", slider.value) * 100) / 100 ;
275.    k = Math.round(find(dataKurzeme, "Years", slider.value) * 100) / 100 ;
276.    z = Math.round(find(dataZemgale, "Years", slider.value) * 100) / 100 ;
277.    r = Math.round(find(dataRiga, "Years", slider.value) * 100) / 100 ;
278.
279.      var regions = [{
280.         "type": "Feature",
281.         "properties": {"reg": "Vidzeme Planning Region","val": v},
282.         "geometry":{
283.           "type":"Polygon",
284.           "coordinates":[[
285.           [27.6905697687,57.3700111292],
286.           [27.6737791733,57.3938946617],
287.    ...
288.
289.              ]]
290.           }}, {
291.         "type": "Feature",
292.         "properties": {"reg": "Zemgale Planning Region","val": z},
```

```
293.          "geometry":{
294.             "type":"Polygon",
295.             "coordinates":[[
296.          …              ]]}
297.        }];
298.
299.      geojson = L.geoJSON(regions, {style: style, onEachFeature: onEachFeature
300.          }).addTo(map);
301.    label()
302.    };
303.
304.    function getColor(d) {
305.      return d > 1   ? '#0c2c84' :
306.          d > 0.6   ? '#225ea8' :
307.          d > 0.5   ? '#1d91c0' :
308.          d > 0.4   ? '#41b6c4' :
309.          d > 0.3   ? '#7fcdbb' :
310.          d > 0.1   ? '#c7e9b4' :
311.                '#deebf7';
312.    };
313.
314.
315.    function style(feature) {
316.      return {
317.        fillColor: getColor(feature.properties.val),
318.        weight: 2,
319.        opacity: 0.5,
320.        fillOpacity: 0.5
321.      };
322.    };
323.
324.    function highlightFeature(e) {
325.      var layer = e.target;
326.
327.      layer.setStyle({
328.        weight: 5,
329.        color: '#666',
330.        dashArray: '',
331.        fillOpacity: 0.7
332.      });
333.
334.      info.update(layer.feature.properties);
335.    };
336.
337.    function resetHighlight(e) {
338.      geojson.resetStyle(e.target);
339.      info.update();
340.    }
341.
342.    function onEachFeature(feature, layer) {
```

```
343.        layer.on({
344.            mouseover: highlightFeature,
345.            mouseout: resetHighlight,
346.        });
347.    }
348.
349.    geojson = L.geoJSON(regions, {style: style, onEachFeature: onEachFeature
350.    }).addTo(map);
351.
352.    var info = L.control();
353.
354.    info.onAdd = function (map) {
355.        this._div = L.DomUtil.create('div', 'info');
356.        this.update();
357.        return this._div;
358.    };
359.
360.    info.update = function (regions) {
361.        this._div.innerHTML = u +  (regions ?
362.            '<br>'+regions.val+' '+ u +'<br>'+ regions.reg + '</b>'
363.            : '');
364.    };
365.
366.    info.addTo(map);
367.
```